

This is an Open Access document downloaded from ORCA, Cardiff University's institutional repository: <https://orca.cardiff.ac.uk/id/eprint/115115/>

This is the author's version of a work that was submitted to / accepted for publication.

Citation for final published version:

D'Agostino, Ilaria, Giacchello, Ilaria, Nannetti, Giulio , Fallacara, Anna Lucia, Deodato, Davide, Musumeci, Francesca, Grossi, Giancarlo, Palù, Giorgio, Cau, Ylenia, Trist, Iuni Margaret, Loregian, Arianna, Schenone, Silvia and Botta, Maurizio 2018. Synthesis and biological evaluation of a library of hybrid derivatives as inhibitors of influenza virus PA-PB1 interaction. *European Journal of Medicinal Chemistry* 157 , pp. 743-758. 10.1016/j.ejmech.2018.08.032

Publishers page: <http://dx.doi.org/10.1016/j.ejmech.2018.08.032>

Please note:

Changes made as a result of publishing processes such as copy-editing, formatting and page numbers may not be reflected in this version. For the definitive version of this publication, please refer to the published source. You are advised to consult the publisher's version if you wish to cite this paper.

This version is being made available in accordance with publisher policies. See <http://orca.cf.ac.uk/policies.html> for usage policies. Copyright and moral rights for publications made available in ORCA are retained by the copyright holders.



Synthesis and biological evaluation of a library of hybrid derivatives as inhibitors of Influenza Virus PA-PB1 interaction.

Ilaria D'Agostino;^{1,#} Ilaria Giacchello;^{2,#} Giulio Nannetti;^{3,#} Anna Lucia Fallacara;¹ Davide Deodato;¹
Francesca Musumeci;² Giancarlo Grossi;² Giorgio Palù;³ Ylenia Cau;¹ Iuni Margaret Trist;¹ Arianna
Loregian;^{3,*} Silvia Schenone;^{2,*} Maurizio Botta.^{1,4,5}

1 Dipartimento di Biotecnologie, Chimica e Farmacia, Università degli Studi di Siena, Via A. Moro, I-53100 Siena, Italy

2 Dipartimento di Farmacia, Università degli Studi di Genova, Viale Benedetto XV, 3, 16132, Genova, Italy

3 Dipartimento di Medicina Molecolare, Università degli Studi di Padova, Via A. Gabelli 63, I-35121 Padova, Italy

*4 Sbarro Institute for Cancer Research and Molecular Medicine, Temple University, BioLife Science Building, Suite 333, 1900 N
12th Street, Philadelphia, Pennsylvania 19122, United States*

5 Lead Discovery Siena s.r.l., Via Vittorio Alfieri 31, I-53019 Castelnuovo Berardenga, Italy

**Corresponding authors: arianna.loregian@unipd.it; schensil@unige.it.*

#These authors equally contributed to the work.

ABSTRACT. The limited treatment options against influenza virus along with the growing public health concerns regarding the continuous emergence of drug-resistant viruses make essential the development of new anti-flu agents with novel mechanisms of action. One of the most attractive targets is the interaction between two subunits of the RNA-dependent RNA polymerase, PA and PB1. Herein we report the rational design of hybrid compounds starting from a 3-cyano-4,6-diphenylpyridine scaffold recently identified as disruptor of PA-PB1 interactions. Guided by the previously reported SAR data, a library of amino acid derivatives was synthesized. The biological evaluation led to the identification of new PA-PB1 inhibitors, that do not show appreciable toxicity. Molecular modeling shed further lights on the inhibition mechanism of these compounds.

KEYWORDS: anti-influenza; PA-PB1; RdRp; amino acid coupling; SPPS; diphenyl-pyridine.

INTRODUCTION. Influenza, also known as flu, is an acute respiratory illness caused by the infection of viruses which belong to the *Orthomyxoviridae* family. These pathogens are enveloped viruses containing a single-stranded, negative-sense and segmented RNA genome and are classified in A, B, C and D,[1,2] according to the antigenicity of their nucleoprotein (NP) and matrix protein 1 (M1).[3] Infections by influenza

ABBREVIATIONS

AcOEt, Ethyl acetate; CC₅₀, Half maximal cytotoxic concentration; cRNA, complementar RNA; DCM, dichloromethane; DDQ, 2,3-Dichloro-5,6-dicyano-1,4-benzoquinone; DIPEA, *N,N*-Diisopropylethylamine; DMEM, Dulbecco's Modified Eagle's Medium; DMF, *N,N*-dimethylformamide; DMSO, *N,N*-dimethylsulfoxide; EC₅₀, Half maximal effective concentration; EDC, 1-Ethyl-3-(3-dimethylaminopropyl)carbodiimide; ELISA, enzyme-linked immunosorbent assay; EtOH, ethanol; FluA, influenza A virus; FluB, influenza B virus; FluC, influenza C virus; Fmoc, Fluorenylmethylloxycarbonyl; GAFF, General Amber Force Field; H₂O, water; HA, hemagglutinin; HBTU, 2-(1H-Benzotriazole-1-yl)-1,1,3,3-tetramethyluronium hexafluorophosphate; HEK, human embryonic kidney; HOBt, Hydroxybenzotriazole; IC₅₀, Half maximal inhibitory concentration; MD, molecular dynamics; MDCK, Madin-Darby canine kidney; MeOH, methanol; mRNA, messenger RNA; MM-GBSA, Molecular Mechanics-Generalized Born Surface Area; MTT, (3-(4,5-Dimethylthiazol-2-yl)-2,5-Diphenyltetrazolium Bromide; MW, microwave oven; N₂, nitrogen; NA, neuraminidase; NaN₃, sodium azide; NaOH, sodium hydroxide; OSV, oseltamivir carboxylate; PA, polymerase acidic protein; PAINs, pan assay interference compounds; PB1, polymerase basic protein 1; PB1_N, *N*-terminal of PB1; PB2, polymerase basic protein 2; PDB, Protein Data Bank; PPI, protein-protein interaction; PRA, plaque reduction assay; RBV, ribavirin; RdRp, RNA-dependent RNA polymerase; RNA, ribonucleic acid; SAR, structure-activity relationship; SD, standard deviation; SI, selectivity index; SOCl₂, thionyl chloride; SPPS, solid phase peptide synthesis; *t*Bu, *tert*-butyl; TFA, trifluoroacetic acid; THF, tetrahydrofuran; TIPS, triisopropylsilyl ether; vRNA, viral RNA.

A (FluA) and B (FluB) virus are the most relevant and occur globally as epidemics (seasonal flu almost every winter) or as more sporadic pandemics caused by always new and very different A viruses. Seasonal flu accounts for a large number of cases worldwide each year (between 9.2 and 35.6 million; 5–10% of adults and 20–30% of children)[4] and can cause severe illness especially in population at high risk for influenza-related complications (e.g. immunocompromised, patients with chronic diseases and paediatric and old people), resulting in hospitalization and death.[5]

Influenza viruses undergo continuous antigenic drifts and sporadic antigenic shifts that result in minor and major antigenic changes of the viral surface glycoproteins and allow the viruses to evade the pre-existing host immune response. For this reason, influenza vaccines must be constantly reformulated and fail to provide protection against novel pandemic strains.[6–8] Only two classes of chemotherapeutics are currently available: the M2-blockers, such as amantadine and rimantadine, that inhibit the replication by blocking the M2 proton channel[9] and the neuraminidase inhibitors, such as zanamivir and oseltamivir, that prevent virus release from infected cells. The increase of chemoresistance,[10–22] the serious side effects of the current anti-flu drugs[23] and the difficulty of production of cross-protective vaccines, make current therapeutic armamentarium limited and poorly effective,[24] molecules to fit.[29,55] After first attempts of PPI inhibition through PB1-derived peptides,[44,51,53,56] several different libraries of small molecules were investigated by *in silico* screenings, biochemical assays and rational design.[50,52,57–65]

In the last few years, our research group identified benzofurazan derivatives as inhibitors of PA–PB1 interaction through high throughput screening (HTS) and these compounds were characterized by an ELISA-based assay followed by plaque reduction assay (PRA) on FluA/WSN/33 (H1N1)-infected MDCK cells. This led us to identify the hit compound **1** (**Figure 1**), showing micromolar antiviral activity ($EC_{50} = 5 \mu\text{M}$), but cytotoxicity in MDCK cells ($CC_{50} = 20 \mu\text{M}$).[66] In order to explore the SARs and improve the selectivity index (SI) and water solubility, a large library of benzofurazan derivatives was synthesized and tested, giving a more potent compound **2** ($IC_{50} = 35 \mu\text{M}$, $EC_{50} = 1 \mu\text{M}$), but still cytotoxic ($CC_{50} = 40 \mu\text{M}$) (**Figure 1**).[67] Despite the good anti-flu activity, this class of compounds was found to be unsuitable for further development because of its poor SI. A model of the PA-PB1 complex was built based on PDB IDs 3CM8[68] and 2ZNL[44] and it was used to perform a MD simulation to identify the hot-spot residues for the inhibition. The following high throughput docking approach (a consensus docking protocol combining Glide[69] and Gold[70] programs)[67] together highlighting the need for new targets discovery and exploitation. Because of its critical role in FluA infection and its high amino acid conservation,[25–28] the viral polymerase is widely recognized as one of the most promising anti-flu targets.[29–32]

The RNA-dependent RNA polymerase (RdRp) is a heterotrimeric complex composed of polymerase acidic protein (PA), polymerase basic proteins 1 and 2 (PB1 and PB2, respectively) with a combined mass of approximately 250 KDa. [33,34] The enzymatic complex is associated to the NP-encapsulated RNA strand to form the viral ribonucleoprotein complex (RNP).[33,35] It plays a key role in the viral life cycle, as it is directly required for both transcription and replication.[25,26,33,36–41] The Flu RdRp cleaves the 5'-methyl cap from the host pre-mRNA and uses this capped structure as a primer for the synthesis of the viral mRNA

by a cap-snatching mechanism. The polymerase complex also catalyses the genome replication, generating a positive-sense complementary RNA (cRNA), a replicative intermediate that serves as a template for the synthesis of more copies of the viral genomic segments (vRNA).[33,34,42,43] The polymerase catalytic site is in PB1; PB2 includes the capped-RNA recognition domain, required for generation of the primer for transcription, while PA is involved in the complex assembly.[42,44–46] Only if correctly assembled RdRp can work and the virus can replicate its genome.[41,44,47,48] Indeed, even if so far the search for new antiviral targets has been mostly focused on the PA endonuclease active site, PB2 cap-binding domain and PB1 subunit,[49] a very attractive strategy could be the disruption of RdRp complex assembly through protein-protein interaction (PPI) inhibition. In fact, PPIs represent crucial events in many biological processes under both physiological and pathological conditions. In particular, crystallization studies have revealed that PA-PB1 interaction may be a very promising druggable target, [29,49–52] because of the high degree of conservation of several interface residues among FluA, FluB and FluC,[27,53,54] that suggests that its inhibitors may be active against many viral subtypes and less prone to drug-resistance, and because of the little size of the specific interface that allows small

with ELISA evaluation revealed the 3-cyano-4,6-diphenyl-pyridine scaffold as a promising potential inhibitor of the PA–PB1 complex by mimicking the hydrophilic *N*-terminal portion of PB1 (residues 1–4) and the most important interactions with the *C*-terminal domain of PA. Compounds **3** and **4** (**Figure 1**), showed the best activity profile.[63] The following validation of the reliability of the old homology model was performed through comparison with the more complete X-ray structure of FluA H17N10 RdRp (PDB ID: 4WSB)[41] and the superposition in the PB1-binding site region.[71] Chemical modifications aided by molecular modeling studies allowed us to make preliminary SAR considerations and to identify some compounds (**5** and **6**, **Figure 1**) as promising anti-flu agents, even if they suffer from low water solubility that implied the design and validation of a new serum-free ELISA.[71]

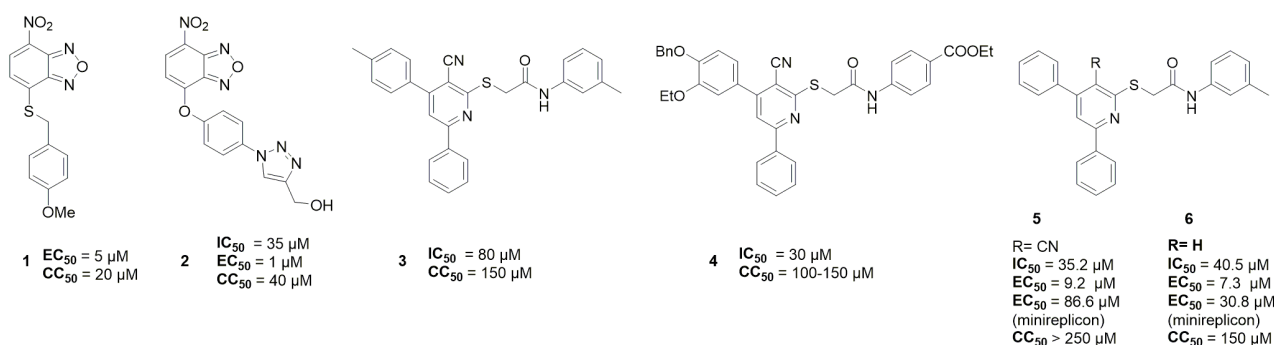


Figure 1. Structures of compounds **1-6** from previous works.[63,66,67,71]

DISCUSSION. The biological evaluation of the compounds described above[71] allowed us to confirm this novel class of diphenyl-pyridine derivatives as promising and non-toxic PA-PB1 disrupting RdRp inhibitors, and to determine preliminary SARs. In order to increase the affinity to the PB1 binding site, a rational design of new derivatives was performed.

As already discussed, this library of derivatives contains a scaffold that directly competes and displaces the *N*-terminal portion of PB1 (PB1_N). Indeed, the overlap of PB1_N in the X-ray crystallography structure with the docking pose of compound **3** (**Figure 2**) revealed that the cyano-pyridine core fits very well with a central region of PB1_N, but the compound fails in establishing crucial interactions instead made with PA by the three terminal amino acids (Met1-Asp2-Val3) of PB1_N peptide.[63,71]

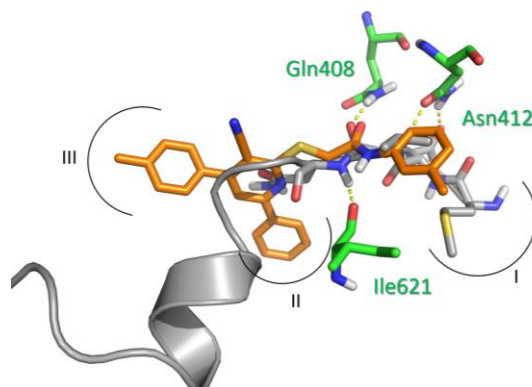


Figure 2. Superimposition of the crystallographic poses of PB1_N and the docking pose of compound **3**, a representative molecule of the cyano-pyridine library, with the interaction protein region I, II and III. PB1_N is shown as grey cartoon and the last three amino acids (Met1-Asp2-Val3) are represented by sticks. The three amino acids of PA (Gln408, Asn412 and Ile621) that interact with the C2 chain are represented by green sticks and labelled.

With the aim to enhance the ability of our compounds to completely displace PB1 and increase their affinity toward the target protein PA, a hybrid derivative, combining the cyano-pyridine core linked to the PB1_N last peptide side chain (Met-Asp-Val) has been designed and docked into the PB1 binding site on PA. The rational design was performed choosing the cyano-pyridine ring of compound **3** as the nucleus to which specific amino acids were added on the C2 side chain. Since the majority of the first virtual screening hits[63] were characterized by a *p*-methyl group substituent on the C4 phenyl ring, this was maintained.

At first, the hybrid **Target Compound** (see structure in **Scheme S1** of *Supplementary information*) was planned with the molecule bearing the peptide as *N*-terminal amine. Despite a lot of attempts (some of which are reported in *Supplementary information*), the synthesis of this first designed **Target Compound** has proven to be difficult to achieve; so we decided to prepare its “inverted amide”, inserting the peptide as *C*-terminal. This modification was shown to be not relevant for the interaction with the most important residues of PA, confirming a sufficiently similar docking pose.

In fact, from docking simulations, emerged that both the first designed **Target Compound** and the compound with the inverted amide **11** (structure reported in **Figure 3-4**) were able to maintain the characteristic interactions of the cyano-pyridine derivatives with Lys643 and Gln408 of PA also establishing two additional hydrogen bonds with Val621 and Asn412 through the backbone of the terminal Asp and Val amino acids (**Figure 3A**). The superimposition of the docking pose of compound **11** binding mode with the PB1_N fragment demonstrated a good overlap of the tripeptide region (**Figure 3B**).

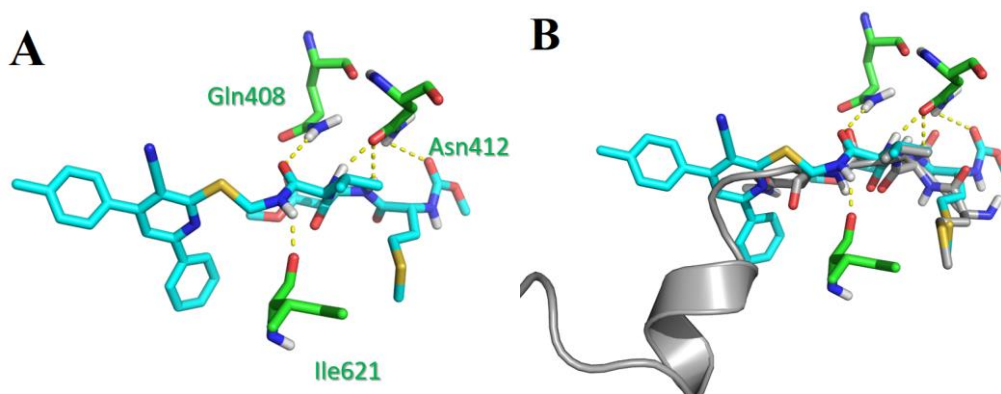


Figure 3. Docking pose of compound **11** in PA (Panel **A**) and superimposition of docking poses of compound **11** and PB1_N (Panel **B**). PA residues are represented by green sticks and PB1_N is represented in grey.

The adducts with valine, valine-aspartate and valine-aspartate-methionine methyl esters (**7a**, **9** and **11** respectively, shown in **Figure 4**) were synthesized in order to explore the chemical space around the C2 side chain. We decided to introduce amino acids as esters because they are more permeable through membranes than the correspondent free acids.[72,73] Compound **11** turned out to be a weak inhibitor, while more interesting activity profiles have been revealed for compounds **7a** and **9**. They showed a relevant discordance between the low PA-PB1 interaction inhibition and the good intracellular activity, but minireplicon assays confirmed the on-target activity (data reported in **Table 1**), suggesting a possible enzymatic hydrolysis in the cell. To confirm this hypothesis, the free acid of Val and Val-Asp adducts were synthesized, through a controlled hydrolysis in basic conditions, yielding **8** and **10** respectively. The biological data of these derivatives seem to confirm that they are the actual responsible for the antiviral activity, as expected. The good results of Val adducts **7a** and **8** are in agreement with experimental data previously reported by Wunderlich et al[74] that revealed Val3 on the PB1 peptide as one of the most important residues for the interaction with PA, exhibiting the lowest binding free energy,[63] thus suggesting that its displacement could inhibit the RdRp heterodimerization.

Encouraged by these findings, we decided to investigate the effects of other amino acids at the protein-protein surface of the target through the addition of different L-amino acids as methyl esters (Leu, Ile, His, Arg, Phe, Tyr, Glu: compounds **7b-h**), whose structures are reported in **Figure 4**, through the validate synthetic procedure of **7a** (**Scheme 2**). Leucine (**7b**) and isoleucine (**7c**) have been chosen as hydrophobic good replacement of valine, while the other residues have been selected as representatives of all the existing classes of amino acids to investigate about the possible interactions of their different functions. Histidine (**7d**) and arginine (**7e**) bear a positive charge at physiological pH, phenylalanine (**7f**) and tyrosine (**7g**) are characterized by aromatic lateral chains that can interact with the protein region I and glutamate (**7h**), if hydrolysed, bears negative charges that could enhance the affinity of ligands towards the protein. Molecular docking studies were then carried out to investigate the possible binding mode of these molecules within the PB1 binding site of PA, while molecular dynamics (MD) simulations were performed to identify the molecular determinants responsible for *in vitro* PA-PB1 PPI inhibition.

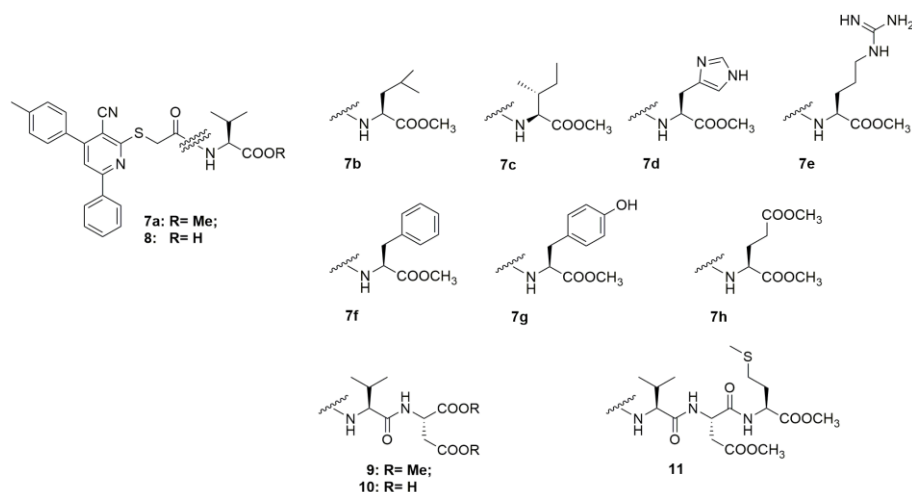
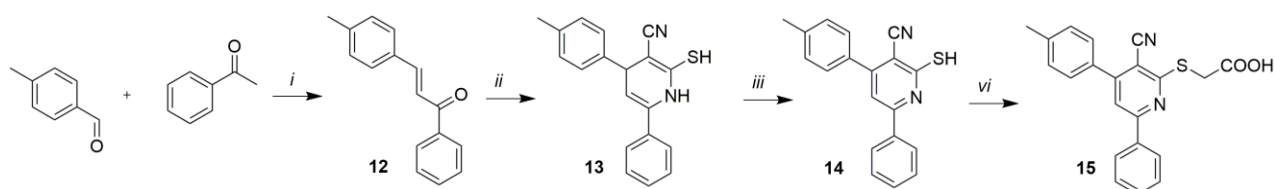


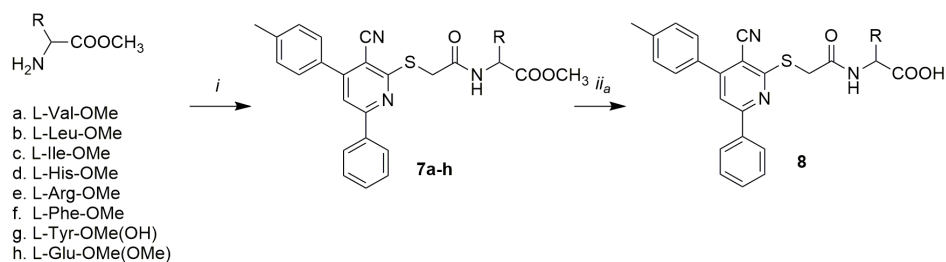
Figure 4. Synthesized hybrid compounds **7-11**.

CHEMISTRY. The first part of the synthetic work has been devoted to the set-up of a fast and high yielding procedure for the preparation of the 4,6-diphenyl-3-cyanopyridinic nucleus. Starting materials were acetophenone and *p*-tolualdehyde which were reacted *via* base catalysed Claisen-Schmidt condensation reaction, affording the chalcone derivative **12**.^[75–77] This acts as Michael acceptor and the dihydropyridine derivative **13** was obtained through a Hantzsch-type cyclization of **12** with cyanothioacetamide using sodium methoxide as a base.^[78] Compound **13** was aromatized with 2,3-dichloro-5,6-dicyano-*p*-benzoquinone (DDQ) affording 2-mercapto derivative **14**.^[79] Then, a nucleophilic substitution of 2-bromoacetic acid was carried out in DMF using potassium hydroxide as base affording the cyano-pyridinic core **15** (**Scheme 1**).



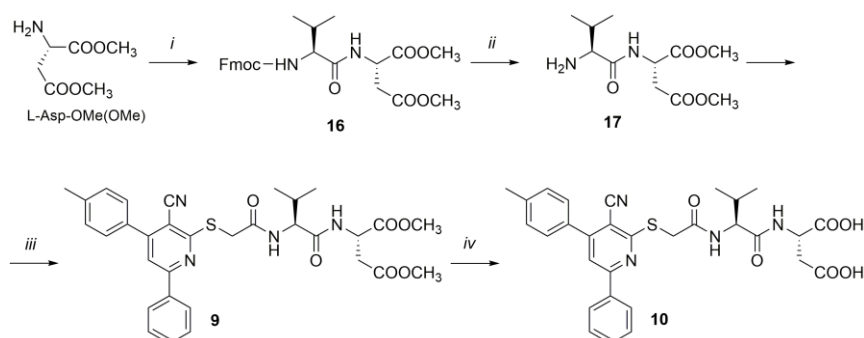
Scheme 1. Synthesis of cyano-pyridinic core. *Reagents and conditions:* (i) NaOH 4N, abs EtOH, N₂, r.t., 2 h; (ii) Cyanothioacetamide, Na⁰, dry MeOH, N₂, ref., 90 min; (iii) DDQ, DCM, r.t., 3 h; (vi) Bromoacetic acid, KOH 10%, DMF, r.t., 4 h.

To synthesize the mono amino acid adducts **7a-h**, we used the same amidation procedure with EDC (1-ethyl-3-(3-dimethylaminopropyl)carbodiimide) and HOBt (hydroxybenzotriazole) as coupling agents^[78] and racemization suppressors,^[80] dry DIPEA (*N,N*-diisopropylethylamine), carboxylic acid **15** and the appropriate amino acid methyl ester in dry DMF. Methyl ester **7a** was hydrolysed in mild basic conditions furnishing the free carboxylic derivative **8** (**Scheme 2**).



Scheme 2. Synthesis of mono-amino acid adducts **7a-h** and **8**. *Reagents and conditions:* (i) **15**, EDC, HOBt, dry DIPEA, dry DMF, N₂, 0 °C to r.t., 3 h; (ii_a) only for **7a**: NaOH 1N, THF/EtOH/H₂O, r.t., 30 min. **R** is the lateral chain of the appropriate amino acid.

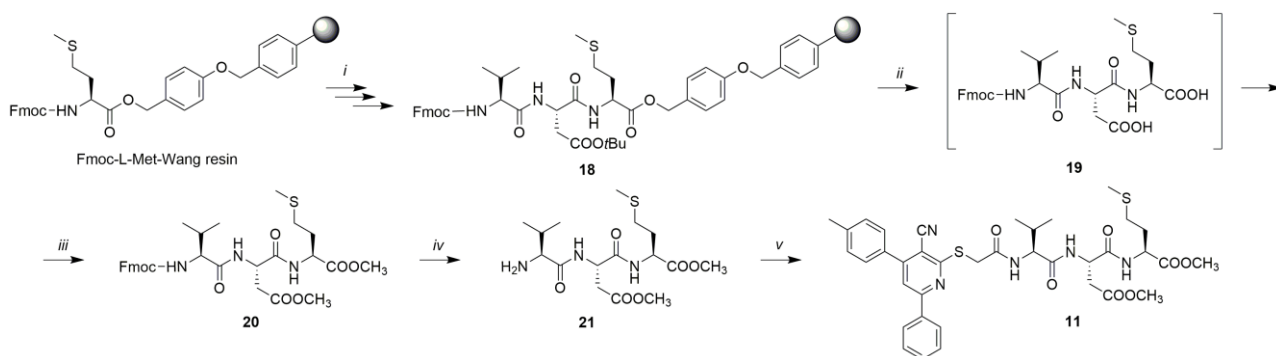
The synthetic route to obtain di-amino acid adduct **9** is shown in **Scheme 3**. The Val-Asp dipeptide **16** was synthesized in solution phase through the previous described amidation procedure with Fmoc-L-valine and L-aspartic acid methyl ester. Dipeptide **16** was subjected to the cleavage of the Fmoc protecting group with sodium azide (NaN₃). The free amine **17** was then coupled with acid derivative **15** furnishing the di-amino acid adduct **9**. Eventually, the ester functions of **9** were hydrolysed by using a sodium hydroxide solution affording the bicarboxylic acid derivative **10**.



Scheme 3. Synthesis of di-amino acid adducts **9** and **10**. *Reagents and conditions:* (i) EDC, HOBt, dry DIPEA, dry DMF, N₂, 0 °C to r.t., 8 h; (ii) NaN₃, DMF, 50 °C, 5 h; (iii) EDC, HOBt, dry DIPEA, dry DMF, N₂, 0 °C to r.t., 4 h; (iv) NaOH 1N, THF/EtOH/H₂O, r.t., 30 min.

The synthesis of the tri-amino acid adduct **11** required the preparation of the tripeptide Val-Asp-Met, that was performed in solid phase through the Fmoc strategy and is reported in **Scheme 4**. MW-SPPS (Microwave Solid Phase Peptide Synthesis) was conducted by using an automated peptide synthesizer, that was charged with a resin (Wang resin) bearing the last amino acid of our tripeptide, L-methionine, covalently linked. Prior to use, the resin was swelled for 2 hours in DMF. In addition to resin and solvents (DMF and DCM), the instrument was also charged with the other two protected amino acids (Fmoc-L-Asp-(*O*tBu) and Fmoc-L-Val), the coupling activators (HOBt and HBTU), a base (DIPEA) and a deprotection solution (20% piperidine in DMF). At the end of the deprotection and coupling cycles, we obtained the resin-bounded tripeptide **18**, which was manually cleaved to avoid the employment of corrosive trifluoroacetic acid (TFA) inside the instrument. The cleavage of the resin was performed through a solution of TFA, H₂O and triisopropylsilane (TIPS) as scavengers for the reactive species produced during resin cleavage, and dithiotreitol (DTT) to avoid methionine oxidation. Under these acid conditions the *tert*-butyl ester in the aspartate lateral chain was

hydrolysed furnishing the resin-free tripeptide **19** which was used in the next step without further purification. Then the methyl esterification of dicarboxylic functions of **19**, accomplished by treating it with a methanolic solution of freshly distilled thionyl chloride (SOCl₂), was necessary to avoid side reactions in next steps. The reaction was carried out at room temperature and with controlled equivalents of SOCl₂ in order not to allow the acid-catalysed racemization of the methionine stereocenter. Dimethyl ester tripeptide **20** was then deprotected from the Fmoc group furnishing the free amine **21** which was coupled with carboxylic core **15** affording the final tri-amino acid adduct **11**.



Scheme 4. Synthesis of tri-amino acid adduct (**11**). *Reagents and conditions:* (i) at Microwave Automated Peptide Synthesizer; (ii) TFA/TIPS/H₂O/DTT, N₂, 3 h; (iii) SOCl₂ dist., dry MeOH, N₂, r.t., 6 h; (iv) NaN₃, DMF, 50 °C, 4 h; (v) **15**, EDC, HOBT, dry DIPEA, dry DMF, 0 °C for 30 min., r.t., 12 h.

BIOLOGY. Amino acid derivatives **7-11**, and the intermediates **15**, **23** and **24** (the synthetic schemes of these last two compounds are reported in *Supplementary Information*) were tested as inhibitors of the PA–PB1 interaction. The *in vitro* biological evaluation of these compounds was conducted through enzyme-linked immunosorbent assays (ELISA) and plaque reduction assays (PRA) in Madin–Darby canine kidney (MDCK) cells infected with FluA virus (A/PR/8/34 strain). The ELISA PA–PB1 interaction assay can measure the physical inhibition between the two subunits, providing IC₅₀ values. This assay was performed using the PB1(1–15)-Tat peptide[56] as a positive control for inhibition. The PRA evaluates the block of the viral replication and includes oseltamivir carboxylic acid (OSV), the active form of oseltamivir (NA inhibitor) and ribavirin (RBV) as positive controls. Cytotoxicity was assessed both in MDCK and in HEK 293T cell lines by MTT assays.

Moreover, to confirm the mechanism of action implied by the ELISA interaction assay, the ability of the most interesting compounds (**7a**, **7c**, **8**, **9**, **15**, **24**) to inhibit FluA RdRp enzymatic activity in a cellular context was assessed by minireplicon assays in transfected HEK 293T cells, using ribavirin (RBV)[81] as a reference drug, since it acts as RNA synthesis inhibitor thanks to its guanosine-like structure. In **Table 1** all the biological data are reported.

The tripeptide derivative (**11**) showed a weak inhibitory activity (IC₅₀ = 68 ± 14 μM) but such an activity is not retained in cells (EC₅₀ > 100 μM in PRA).

The biological data for the methyl esters **9** and **7a**, in particular the minireplicon assay results for **7a**, confirmed our hypothesis of a possible intracellular hydrolysis, so one could assume that their actual target is the PA-PB1

interaction, considering similar or lower EC_{50} values in minireplicon assays when compared to the ones observed in PRAs.

In fact, the free acid adduct **10** inhibited the interaction between PA and PB1 with a IC_{50} value of $77\pm 9\ \mu\text{M}$, while it was less active in blocking viral replication in infected cells ($EC_{50} = 100\ \mu\text{M}$ in PRA), likely due to its inability to pass through the membranes. In contrast, the correspondent methyl ester **9** exhibited a good activity in cell, according to PRA and minireplicon results ($EC_{50} = 49\pm 8\ \mu\text{M}$ and $EC_{50} = 59\pm 18\ \mu\text{M}$, respectively), but a low ability to disrupt the PA-PB1 interaction in ELISA ($IC_{50} = 143\pm 1\ \mu\text{M}$).

As far as the valine adducts, the methyl ester derivative **7a** seemed to have a similar biological profile than the di-peptide adduct **9**, showing a good antiviral activity ($EC_{50} = 52\pm 2\ \mu\text{M}$ in PRA) and confirming the on-target activity in minireplicon assays ($EC_{50} = 41\pm 16\ \mu\text{M}$), while a high IC_{50} value of $167\pm 20\ \mu\text{M}$ was detected. The free acid derivative **8** showed similar EC_{50} values in PRA and in minireplicon experiments (50 ± 7 and $77\pm 14\ \mu\text{M}$, respectively) and a more potent activity in ELISA ($IC_{50} = 76\pm 16\ \mu\text{M}$) when compared to its methyl ester correspondent **7a**.

Surprisingly, although the small difference in the side chain, leucine (**7b**) and isoleucine (**7c**) adducts were found to have very different biological profiles: **7b** appeared to have a low ability to disrupt the PA-PB1 interaction ($IC_{50} = 149\pm 15\ \mu\text{M}$), but showed a weak inhibitory activity in infected cells ($EC_{50} = 97\pm 9\ \mu\text{M}$); while **7c** had a very promising antiviral activity in infected cells ($EC_{50} = 39\pm 2\ \mu\text{M}$ in PRA) and likely acted by inhibiting the PA-PB1 PPI, as suggested by both the ELISA ($IC_{50} = 36\pm 3\ \mu\text{M}$) and the minireplicon assays ($EC_{50} = 53\pm 16\ \mu\text{M}$). The histidine derivative (**7d**) resulted to have good activity in the ELISA experiments ($IC_{50} = 32\pm 7\ \mu\text{M}$), but, unfortunately, a high cytotoxicity was detected ($CC_{50} = 152\pm 3\ \mu\text{M}$ in MDCK cells). The arginine and the tyrosine adducts (**7e** and **7g** respectively) were effective as disruptors of the target interaction, with IC_{50} values of 48 ± 8 and $18\pm 5\ \mu\text{M}$, respectively, but did not retain the antiviral activity in cells ($EC_{50} > 100\ \mu\text{M}$). A particular case is the one of the phenylalanine derivative (**7f**) that seems not to have affinity with PA ($IC_{50} > 200\ \mu\text{M}$), but in infected cells was active with an EC_{50} value of $68\pm 10\ \mu\text{M}$ in PRA, perhaps after the ester hydrolysis or through an off-target mechanism of action. At the end, the glutamate derivative (**7h**) is found to be inactive.

All tested compounds were non cytotoxic in MDCK and HEK 293T cells ($CC_{50} > 200\ \mu\text{M}$) apart from **7d**.

Comparing our best compound (**7c**) to the previous published compound **5**, we can observe a similar ability to disrupt the PA-PB1 interaction in ELISA. Moreover, even if compound **5** is a very potent antiviral agent with an EC_{50} of $9.2\pm 0.7\ \mu\text{M}$ in PRA, its activity is probably due to other additional modes of action as revealed by minireplicon assays ($EC_{50} = 86.6\pm 15\ \mu\text{M}$).

The intermediates **15**, **23**, **24** (the structures of the two last compounds are reported in *Supplementary Information*) were also tested: while the amine **23** resulted inactive, the acid **15** and the amide **24** showed interesting activity profiles, even if a low toxic behaviour in HEK 293T cell line was detected.

Table 1. Biological profiles of the synthesized compounds **7-11**, **15**, **23** and **24**.

Compound	ELISA PA-PB1 IC ₅₀ [μM] ^{a,e}	PRA in MDCK cells EC ₅₀ [μM] ^{b,e}	MTT in MDCK cells CC ₅₀ [μM] ^{c,e}	Minireplicon Assay EC ₅₀ [μM] ^{d,e}	MTT in HEK 293T cells CC ₅₀ [μM] ^{c,e}
7a	167 ± 20	52 ± 2	210 ± 8	41 ± 16	> 250
7b	149 ± 15	97 ± 9	215 ± 28	-	-
7c	36 ± 3	39 ± 2	>250	53 ± 16	229 ± 12
7d	32 ± 7	80 ± 6	152 ± 13	-	-
7e	48 ± 8	>100	>250	-	-
7f	>200	68 ± 10	240 ± 18	-	-
7g	18 ± 5	>100	>250	-	-
7h	187 ± 14	>100	>250	-	-
8	76 ± 16	50 ± 7	> 250	77 ± 14	250
9	143 ± 17	49 ± 8	> 250	59 ± 18	> 250
10	77 ± 9	100	> 250	-	-
11	68 ± 14	>100	> 250	-	-
15	56 ± 5	65 ± 11	> 250	43 ± 14	218 ± 21
23	>200	> 100	> 250	-	-
24	102 ± 18	41 ± 5	> 250	65 ± 14	218 ± 21
5 ⁷¹	35.2 ± 5.1	9.2 ± 0.7	>250	86.6 ± 15.0	> 250
PB1₍₁₋₁₅₎-Tat peptide	31.7 ± 10.8	49.7 ± 5.1	> 250	15.5 ± 2.6	> 250
OSV	-	0.015 ± 0.006	> 250	-	> 250
RBV	-	12.8 ± 2.1	> 250	23.8 ± 4.5	> 250

-: not determined. ^aActivity of the compounds in the ELISA PA–PB1 interaction assay. Values represent the compound concentration (in μM) that reduces the interaction between PA and PB1 by 50% (IC₅₀). ^bAntiviral activity of the compounds in plaque reduction assays against the Flu A/PR/8/34 strain. Values represent the compound concentration (in μM) that inhibits 50% of plaque formation (EC₅₀). Compound concentrations higher than those reported could not be tested in PRA due to cytotoxicity. ^cCytotoxicity of the compounds exhibited in MTT assays. Values represent the compound concentration (in μM) that causes a 50% decrease in cell viability (CC₅₀). The CC₅₀ were assessed in MDCK and HEK 293T cells. ^dThe EC₅₀ values represent the compound concentration that reduces by 50% the activity of FluA virus RNA polymerase in HEK 293T cells. ^eAll values represent the means ± SD of data derived from at least three independent experiments in duplicate. Reference compounds are the previous described compound **5**, PB1₍₁₋₁₅₎-Tat peptide, oseltamivir carboxylic acid (OSV) and ribavirin (RBV).

MOLECULAR MODELING. The ELISA PA–PB1 interaction assay provided a direct measure of the PA-PB1 PPI inhibition by test compounds. Here, to add further insights into the inhibition mechanism, we carried out molecular modeling investigations. First, the possible binding mode of compounds listed in **Table 1** to the PB1 binding site of PA was predicted by molecular docking, which was performed with the GOLD program (GoldScore function)[82] according to previous works.[63,71] Notably, all compounds and intermediates showed to fit the PB1 site of PA with a binding geometry that is highly comparable each other, as well as to the binding mode already described above for compound **11** and the reference inhibitor PB1_N (see **Figure 2**

and **Figure 3**). The binding mode of tested compounds is described in *Supplementary information*. However, probably because of the narrow activity range observed in the ELISA assay (**Table 1**), any attempt to correlate the ligands' scores with experimental data was unsuccessful (*data not shown*). Therefore, to identify the possible molecular determinants responsible for strong inhibition in the ELISA assay, we carried out molecular dynamics (MD) investigations on the docking-based complexes between PA and compounds **7g** and **7f** (**Figure 4**). Indeed, these two molecules differ each other only for the –OH phenol group in **7g** (L-Tyr residue) that is missing in **7f** (L-Phe residue), but were notably different in the ELISA experiment, as **7g** proved the most potent PA-PB1 inhibitor of the tested set while **7f** was inactive up to 200 μM concentration. Thus, they represent a suitable model system to challenge MD simulations. The representative docking complex of **7g** and **7f** was solvated in a box of water molecules and was energy minimized, heated and equilibrated in density as described previously,[83,84] before to run 250 ns of unrestrained MD simulations. Cluster analysis performed on the whole MD production trajectories coupled with visual inspection clearly indicated that **7g** is stable in the PB1 binding site, with a conformation that is highly consistent to that identified by molecular docking (**Figure 5A**). The nitrile group of **7g** establishes a H-bond interaction with the side chain of Lys643 (to allow comparison with results described in previous works [63, 71] residue numbering follows the sequence of A/Wilson-Smith/1933 H1N1 strain). The two phenyl rings of the 3-cyano-4,6-diphenylpyridine scaffold are included in a hydrophobic cleft bounded by Pro625, Phe658, Leu666, Trp706, Phe707, and Phe710. The peptide moiety notably overlaps with the crystallographic pose of the *N*-terminal end of PB1,[26] and establishes a network of H-bonds. First, the amide bond contacts Glu623, and Gln408 (bridged by a water molecule, see **Figure 5A**) that was already highlighted in prior works [63, 71] as a crucial residue for the binding of PA-PB1 inhibitors. The L-Tyr side chain of **7g** is accommodated in a hydrophobic sub-pocket of PA where it interacts with Asn412 (bridged by a water molecule), Ser415, and Lys635. It is worth mentioning that these three H-bonds are established by the –OH phenol group of **7g**, which is missing in **7f**. Different from the docking pose (*Supplementary information*), the peptide moiety of **7f** bends back towards the hydrophobic cleft of PA thus assuming a bad placement as described previously (**Figure 5B**).[71] Moreover, in this conformation **7f** is unable to establish most of H-bond interactions with PA key residues with the only exception of a single H-bond to Lys635. The different binding conformation and interaction network between these two compounds might explain their opposite behaviour observed in the PA–PB1 interaction assay (ELISA). To further substantiate this hypothesis, we estimated the ligand's theoretical affinity by means of the MM-GBSA approach.[85] Delta energy calculations clearly showed that the different binding conformation is associated to a significantly different theoretical affinity, as reported in **Table 2**, which suggests that ligand affinity is mainly related to enthalpy contributions. In summary, this molecular modeling investigation added further insights to the inhibition mechanism of tested molecules and might drive the design of ligands with enhanced affinity for PA.

Table 2. Delta energy of binding of **7g** and **7f** to PA estimated by the MM-GBSA approach.

Compound	MM-GBSA (kcal/mol) \pm SEM ^a
7g	-40.78 \pm 1.12
7f	-27.65 \pm 0.78

^aStandard Error of the Mean

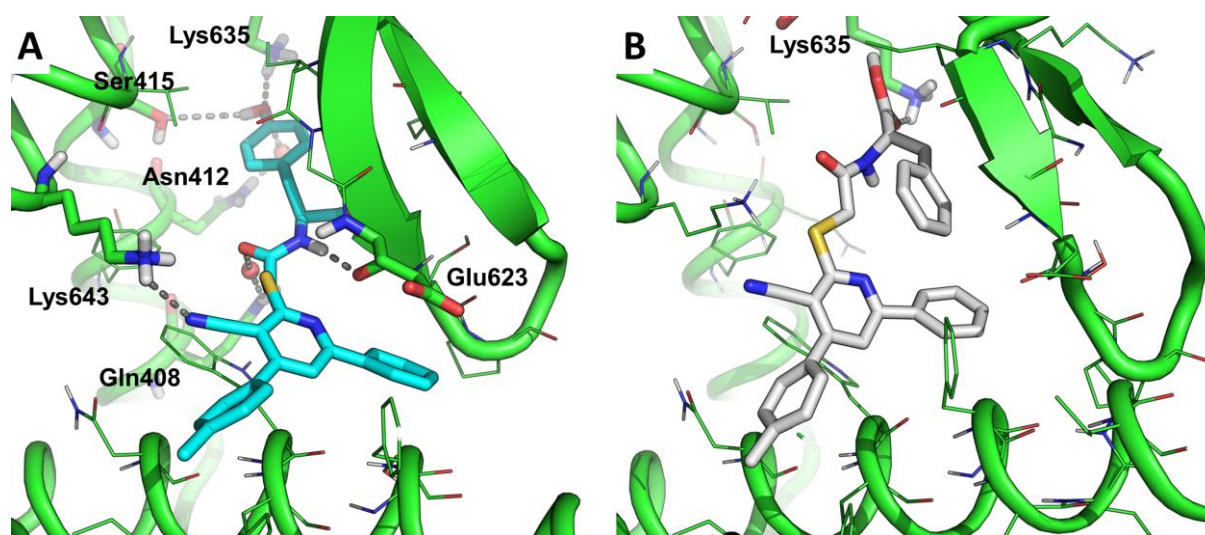


Figure 5. Binding pose of **7g** (panel A) and **7f** (panel B) extrapolated from the most representative cluster of MD frames. The protein is shown as green cartoon, residues within 4 Å from the ligand are showed as lines, residues H-bonded to the ligand are showed as sticks and are labelled. Non-polar H atoms are omitted. Bridged water molecules are showed as red spheres, while the bulky solvent is omitted. **7g** is shown as cyan sticks, **7f** as white sticks. H-bond interactions are highlighted by grey dashed lines.

CONCLUSIONS. In the frame of the limited armamentarium of drugs for the treatment of Flu infections together with the chemo-resistant phenotypes increasing, the search for novel antivirals with innovative mode of action became imperative. In recent years, the viral polymerase has proved to be an attractive target for drug design, although the current efforts led to quite toxic compounds. In particular, some research groups have been interested in the development of small molecules able to interfere with the correct assembly of RdRp complex, through the inhibition of the interaction between PA and PB1, two of its subunits. In this work, starting from previously published findings, a rational drug design led us to synthesize hybrid compounds characterized by the diphenyl-pyridine nucleus, identified as promising inhibitor of the above mentioned PPI, and the same last amino acids side chain of PB1_N (Met-Asp-Val) in C2. Indeed, we planned the synthesis of the tri-peptidic (**11**), di-peptidic (Val-Asp, **9**) and the mono-amino acid (Val, **7a**) derivatives as methyl esters to ensure a higher passive membrane permeability. Biological data results highlighted a major anti-flu activity (EC₅₀ in PRA) of **9** and **7a**, not correlated to the low enzymatic inhibition (IC₅₀ in ELISA). To better investigate this discrepancy, minireplicon experiments were performed, allowing us to confirm the PA-PB1 interaction disruption as the main target of our compounds. Moreover, we hypothesize that these methyl ester derivatives

could be hydrolysed in cell, giving the corresponding free acids. In fact, the synthesized **10** and **8** (free acid dipeptide and mono-amino acid derivatives, respectively) showed a better IC₅₀ when compared to that of **9** and **7a**. Notably, valine derivatives **7a** and **8** emerged as new hit compounds for further optimization. Aimed by the exploration of the chemical space around the C2 of the diphenyl-pyridine core, novel mono-amino acid derivatives (**7b-h**) were synthesized and tested. Interestingly, the modulation in C2 of the starting chemical structures led to an increase in the on-target activity. In particular, the best results were achieved with the isoleucine derivative (**7c**) that exhibited a good biological profile with no cytotoxic behaviour. Molecular modeling simulations added further insights to the inhibition mechanism of these compounds, showing that enthalpy contributions (i.e. H-bond interactions with PA key residues) are crucial to achieve strong PA-PB1 PPI inhibition *in vitro*. In summary, a new small library of hybrid derivatives endowed with anti-influenza activity was generated. Almost of all of these compounds were found to be not cytotoxic at high concentrations in the two cell lines used for testing and to inhibit actually the studied PPI. Moreover, we set up a quantitative four-step scaling-up procedure to synthesize the diphenyl-pyridine scaffold that might be helpful to expand the chemical class and to improve the inhibitory activity.

MATERIAL AND METHODS

1. COMPUTATIONAL SECTION

The crystallographic structure of Influenza A virus PA (C-terminal region) in complex with PB1_N coded by PDB ID: 4WSB,[44] which was already validated as docking receptor in a previous work, [71] was used as rigid receptor in molecular docking studies.[26] Tested compounds were designed by means of Maestro program, and docked by using the GOLD docking program with the GoldScore function.[82] The receptor's site was centred on the carbon atom in position 2 of the indole ring of Trp706, and had a radius of 18 Å. The search efficiency of the Genetic Algorithm was increased up to 200%, while all other parameters were kept at their default values. MD simulations were carried out with Amber16, using the FF14SB force field for the protein and GAFF force field for small molecules.[86] Ligands partial charges were assigned at the am1-bcc level of theory. Each PA-ligand complex was solvated in a rectilinear box of TIP3P water molecules buffering 8 Å from the protein surface. Na⁺ counter-ions were added to neutralize the total charge of the system. First, the water solvent was energy minimized for 500 steps with the steepest descent algorithm (SD) and 1500 steps with the conjugate gradient algorithm (CG); then, the whole system was energy minimized for 1000 steps SD and 4000 steps CG before to be heated up to 300 K in 100 ps (time-step is 2 fs). The heated system was equilibrated in density at constant pressure for 100 ps before to run an equilibration MD at constant pressure for 50 ns. Subsequently, unrestrained MD production was run for 250 ns at constant pressure. Analysis of MD trajectories, including cluster analysis, was carried out by *cpptraj*. [86] Graphics representations were drawn for clusters being representative of more than 60% of MD frames.

2. CHEMISTRY SECTION

All commercially available chemicals and solvents were used as purchased (Merck-Sigma Aldrich, Alfa-Aesar). Anhydrous reactions were run under a positive pressure of dry nitrogen. Anhydrous solvents were prepared by distillation over the appropriate agent: DCM was dried over sodium hydride; THF was dried over sodium and benzophenone; MeOH and EtOH were dried over iodide and magnesium. Anhydrous DMF was used as purchased. Microwave reactions were conducted using a CEM Discover Synthesis Unit (CEM Corp., Matthews, NC). Chromatographic separations were performed on columns packed with silica gel (230-400 mesh, for flash technique). TLC (thin layer chromatography) was carried out using Merck TLC plates silica gel 60 F₂₅₄. Melting points (Mp) were determined with a Büchi B-540 apparatus and are uncorrected. ¹H NMR and ¹³C NMR spectra were recorded at 400 and 100 MHz respectively on a Bruker AC200F spectrometer and are reported in parts per million (δ scale) and internally referenced to the CDCl₃, CD₃OD or DMSO D₆ signal, respectively at δ 7.26 ppm, 3.31 ppm and 2.50 ppm. Chemical shifts for carbon are reported in parts per million (δ scale) and referenced to the carbon resonances of the solvent (CDCl₃ at δ 77.16, CD₃OD at δ 49.00 ppm and DMSO D₆ at 39.52 ppm). Data are shown as following: chemical shift, multiplicity (s = singlet, d = doublet, t = triplet, m = multiplet and/or multiplet resonances, b = broad), coupling constant (*J*) in Hertz (Hz) and integration. Mass spectra (LC-MS) were acquired using an Agilent 1100 LC-MSD VL system (G1946C) by direct injection with a 0.4 mL/min flow rate using a binary solvent system of 95/5 CH₃OH/H₂O. UV detection was monitored at 254 nm. Mass spectra were acquired in positive mode scanning over the mass range 105-1500 *m/z*, using a variable fragmentor voltage of 10-70 mV. IR spectra were measured in KBr with a Perkin-Elmer 398 spectrophotometer. Elemental analysis for C, H, N and S was determined using Thermo Scientific Flash 2000 and results were within $\pm 0.4\%$ of the theoretical value. The purity of final products (**7-11**, **15**, **23** and **24**) was 90% or higher and it was assessed by HPLC-MS, using a Kinetex EVO C18 column (00F-4633-EO: 150 x 4.6 mm, 5 μ m particle size) at a flow rate of 0.6 mL/min with an isocratic elution 60/50 v/v CH₃CN/H₂O (formic acid 0.5% v/v). UV detection was monitored at 254 nm. Mass spectra were acquired in positive mode scanning over the mass range 105-1500 *m/z*, using a fragmentor voltage of 0 mV. The MW-SPPS was performed using Fmoc strategy on a LibertyTM Microwave Peptide Synthesizer (CEM Corporation, Matthews, NC), an additional module of DiscoverTM (CEM Corporation, Matthews, NC) on a 0.10 mmol scale. Wang resin served as the solid support. It was preloaded with the first protected amino acid at a degree of functionalization of 0.60 mmol per gram of resin. The coupling was performed in DMF and the peptide chain assembled under computer control of the synthesizer. The synthesis cycles were composed of Fmoc-deprotection and coupling, both under microwave irradiation. The deprotection was performed with 20% piperidine in DMF, the coupling mixture contained Fmoc-protected amino acid the activating agents HOBt (1-Hydroxybenzotriazole) and HBTU (*O*-(benzotriazol-1-yl)-*N,N,N',N'*-tetramethyluronium tetrafluoroborate) 0.5 M in DMF and an excess of DIPEA (diisopropylethylamine) 34.8% v/v in DMF as the base. The final cleavage of the tripeptide from the solid support and the ester deprotection of the side chains was performed with 88% trifluoroacetic acid (TFA), 5% water, 2% triisopropylsilane (TIS) and 5% DL-Dithiothreitol (DTT) to quench reactive intermediates under microwave irradiation and to prevent the oxidation of the thioether side

chain of methionine. The C-terminal end and the carboxylic aspartate side chain of the peptide is obtained as free carboxylic acids. All parameters (t, p, T, Q) have been established automatically by the instrument and are different in every cycle.

2.1 Synthetic procedures for the acid core 15.

(E)3-(4-Methylphenyl)-1-phenylpro-2-en-1-one (12)

To a stirred solution of acetophenone (3.8 mL; 33.0 mmol) in absolute EtOH (50 mL), a solution of *p*-tolualdehyde (3.8 mL; 33.0 mmol) in dry EtOH (50 mL) and a 4 N aqueous solution of NaOH (20.6 mL) were added. The mixture was stirred at room temperature for 6 h. The reaction was quenched with HCl 2 N and filtered, then the solvent was partially evaporated under vacuum. The residue was dissolved in AcOEt, washed with water, dried over Na₂SO₄, filtered and concentrated under reduced pressure. The solid obtained was decanted with EtOH furnishing the pure chalcone as a pale yellow solid. **TLC R_f** (Hexane/AcOEt 1/6) 0.70. **Yield** 99%. **Mp**: 189-190 °C. **¹H-NMR** (400 MHz CDCl₃): δ (ppm) 7.97 (d, 2H, *J* = 7.6 Hz), 7.80 (d, 1H, *J* = 15.6 Hz), 7.53 (m, 6H), 7.22 (d, 2H, *J* = 7.6 Hz), 2.38 (s, 3H). **¹³C-NMR** (100 MHz CDCl₃): δ (ppm) 190.27, 144.74, 140.96, 138.29, 132.60, 132.09, 129.65, 128.52, 128.46, 128.43, 120.94, 21.45. **LRMS (ESI)** *m/z* = 222.9 [M+H]⁺ ; 244.9 [M+Na]⁺ . **IR** (KBr): cm⁻¹ 3022 (CH=CH), 1656 (CO). **Anal. calcd.** for C₁₆H₁₄O: C 86.45, H 6.35; **found**: C 86.47, H 6.45.

4-(4-Methylphenyl)-6-phenyl-2-sulfanyl-1,4-dihydropyridine-3-carbonitrile (13)

To a solution of sodium (186 mg, 8.10 mmol) in dry MeOH (22 mL) under N₂ atmosphere, chalcone **12** (900 mg, 4.05 mmol) and thiocyanacetamide (405 mg, 4.05 mmol) were added. The mixture was stirred at reflux for 90 minutes. After cooling, the mixture was quenched with HCl 1 N and partially evaporated under vacuum. The residue was diluted in DCM, washed with water, dried over Na₂SO₄, filtered and concentrated under reduced pressure. The pure yellow solid obtained was used directly in the next step. **TLC R_f** (Hexane/AcOEt 4/1) 0.65. **Yield** 94%. **Mp**: 105-133 °C. **¹H-NMR** (400 MHz CDCl₃): δ (ppm) 9.21 (s, 1H), 7.46 (m, 5H), 7.19 (m, 4H), 5.92 (m, 0.4H), 5.78 (m, 0.6H), 4.33 (m, 0.4H), 4.09 (m, 0.6H), 2.35 (s, 3H), 2.04 (s, 1H). **¹³C-NMR** (100 MHz): δ (ppm) 137.38, 132.95, 129.91, 129.74, 129.21, 128.04, 127.52, 125.34, 116.26, 108.90, 108.64, 49.13, 48.38, 42.15, 21.04. **LRMS (ESI)** *m/z* = 304.9 [M+H]⁺; 326.8 [M+Na]⁺. **IR** (KBr) cm⁻¹: 3203 (NH), 2196 (CN). **Anal. calcd.** for C₁₉H₁₆N₂S: C 74.97, H 5.30, N 9.20, S 10.53; **found**: C 74.86, H 5.68, N 8.84, S 10.73.

4-(4-Methylphenyl)-6-phenyl-2-sulfanylpyridine-3-carbonitrile (14)

To a stirred solution of **13** (679 mg, 2.23 mmol) in DCM (15 mL), DDQ (1014 mg, 4.46 mmol) was added. The mixture was stirred at room temperature for 3 h. The mixture was filtered and evaporated under reduced pressure. The dark solid obtained was decanted several times with MeOH, water and hexane to remove DDHQ. The solid was then recrystallized from MeOH. **TLC R_f** (Hexane/AcOEt 4/1) 0.43 **Yield**: 84%. **Mp**: 204-207 °C. **¹H-NMR** (400 MHz CDCl₃): δ (ppm) 7.96 (d, 2H, *J* = 8.0 Hz), 7.61 (s, 1H), 7.53 (d, 2H, *J* = 8.0 Hz), 7.37 (m, 5H), 2.46 (s, 3H), 1.56 (s, 1H). **¹³C-NMR** (100 MHz CDCl₃): δ (ppm) 160.57, 158.83, 154.86, 142.72, 140.58, 136.74, 132.85, 130.64, 129.76, 128.82, 128.27, 127.32, 117.35, 115.48, 21.31. **LRMS (ESI)** *m/z* =

302.9 [M+H]⁺. **IR** (KBr) cm⁻¹: 2215 (CN). **Anal. calcd.** for C₁₉H₁₄N₂S: C 75.47, H 4.67, N 9.26, S 10.60; **found**: C 75.24, H 4.38, N 9.57, S 10.58.

2- {[3- Cyano- 4- (4- methylphenyl)- 6- phenylpyridin- 2- yl]sulfanyl}acetic acid (**15**)

To a stirred solution of **14** (418 mg, 1.38 mmol) in DMF (6 mL) a 10% aqueous solution of KOH (1.70 mL, 3.04 mmol) and a solution of 2-bromoacetic acid (212 mg, 1.52 mmol) in DMF (1 mL) were added and the mixture was stirred at room temperature for 3 h. The mixture became dark red. Then the reaction was treated with HCl 3 N, becoming yellow, and extracted with AcOEt. The organic phase was washed with water, dried over Na₂SO₄, filtered and concentrated under reduced pressure. The crude residue was purified through recrystallization from MeOH to give compound **15** as yellow crystal. **TLC R_f**(AcOEt/MeOH 9/1) 0.43. **Yield**: 75%. **Mp**: 218-220 °C. **¹H-NMR** (400 MHz DMSO D₆): δ (ppm) 8.25 (m, 2H), 7.88 (s, 1H), 7.65 (d, 2H, *J* = 8.0 Hz), 7.51 (m, 3H), 7.39 (d, 2H, *J* = 8.0 Hz), 4.15 (s, 2H), 2.40 (s, 3H). **¹³C-NMR** (100 MHz DMSO): δ (ppm) 170.29, 162.50, 158.40, 154.56, 140.47, 137.01, 133.11, 131.16, 129.84, 129.25, 128.97, 128.05, 116.44, 116.12, 102.81, 33.37, 21.27. **LRMS (ESI)**: *m/z* = 360.9 [M+H]⁺; 382.8 [M+Na]⁺; 398.9 [M+K]⁺. **IR** (KBr) cm⁻¹: 3200-2400 (OH), 2219 (CN), 1710 (CO). **Anal. calcd.** for C₂₁H₁₆N₂O₂S: C 69.98, H 4.47, N 7.77, S 8.90; **found**: C 69.73, H 4.78, N 8.13, S 8.51.

2.2. Synthetic procedure for monoamino acid adducts (**7a-h** and **8**)

General procedure for monoamino acid adducts (**7a-h**)

To a stirred solution of **15** (50 mg, 0.14 mmol) in dry DMF (0.5 mL) at 0 °C under N₂ atmosphere, the appropriate L-amino acid methyl ester (0.15 mmol), EDC (27 mg, 0.14 mmol), HOBT (19 mg, 0.14 mmol) and dry DIPEA (0.03 mL, 0.20 mmol) were added. The mixture was stirred 30 min at 0 °C and then 5 h at room temperature. The reaction was quenched with water and then extracted with AcOEt. The organic phase was washed with water, dried over Na₂SO₄, filtered and concentrated under reduced pressure. The crude residue was purified through flash chromatography on silica gel.

Methyl (2S)- 2- (2- {[3- cyano- 4- (4- methylphenyl)- 6- phenylpyridin- 2- yl]sulfanyl}acetamido)- 3- methylbutanoate (L-Valine methyl ester adduct, **7a**)

Eluted with Hexane/AcOEt 3/1. **Yield**: 20%. White solid. **¹H-NMR** (400 MHz CDCl₃): δ (ppm) 8.05 (m, 2H), 7.60 (s, 1H), 7.53 (m, 5H), 7.35 (d, 2H, *J* = 7.6 Hz), 7.17 (d, 1H, *J* = 6.4 Hz), 4.48 (m, 1H), 4.08 (q, 2H, *J* = 16 Hz), 3.53 (s, 3H), 2.44 (s, 3H), 1.97 (m, 1H), 0.69 (d, 3H, *J* = 6.8 Hz), 0.62 (d, 3H, *J* = 6.8 Hz). **¹³C-NMR** (100 MHz CDCl₃): δ (ppm) 167.92, 161.62, 158.97, 154.90, 140.65, 136.74, 132.83, 130.74, 129.75, 129.03, 128.22, 127.39, 116.52, 115.36, 103.79, 57.34, 51.84, 33.89, 30.87, 29.59, 21.29, 18.60, 17.43. **LRMS (ESI)** *m/z* = 474.7 [M+H]⁺ ; 496.8 [M+Na]⁺. **IR** (KBr) cm⁻¹: 3359 (NHCO), 2220 (CN), 1749 (CO ester), 1646 (CO amide). **Anal. calcd.** for C₂₇H₂₇N₃O₃S: C 68.48, H 5.75, N 8.87, S 6.77; **found**: C 68.37, H 5.59, N 8.77, S 6.64.

Methyl (2S)- 2- (2- {[3- cyano- 4- (4- methylphenyl)- 6- phenylpyridin- 2- yl]sulfanyl}acetamido)- 4- methylpentanoate (L-Leucine methyl ester adduct, 7b)

Eluted with AcOEt/MeOH 9/1. **Yield:** 31%. White solid. **Mp:** 150-151 °C. **¹H -NMR** (400 MHz CDCl₃): δ (ppm) 8.06 (d, 2H, *J* = 7.6 Hz), 7.60 (s, 1H), 7.52 (m, 5H), 7.34 (d, 2H, *J* = 7.6 Hz), 7.13 (d, 1H, *J* = 8.0 Hz), 4.56 (m, 1H), 4.05 (q, 2H, *J* = 15.6 Hz), 3.54 (s, 3H), 2.44 (s, 3H), 1.40 (m, 2H), 1.26 (m, 1H), 0.31 (d, 3H, *J* = 11.4 Hz), 0.27 (d, 3H, *J* = 11.4 Hz). **¹³C-NMR** (100 MHz CDCl₃): δ (ppm) 172.73, 167.71, 161.64, 158.87, 154.90, 140.66, 136.65, 132.82, 130.81, 129.78, 129.07, 128.20, 127.37, 116.43, 103.77, 52.02, 50.81, 41.12, 33.85, 24.53, 22.50, 21.50, 21.31. **LRMS (ESI)** *m/z* = 407.7 [M+H]⁺ ; 509.8 [M+Na]⁺; 525.5 [M+K]⁺. **IR** (KBr) cm⁻¹: 3362 (NHCO), 2222 (CN), 1745 (CO ester), 1650 (CO amide). **Anal. calcd.** for C₂₈H₂₉N₃O₃S: C 68.97, H 5.99, N 8.62, S 6.58; **found:** C 69.01, H 5.87, N 8.50, S 6.53.

Methyl (2S,3S)- 2- (2- {[3- cyano- 4- (4- methylphenyl)- 6- phenylpyridin- 2- yl]sulfanyl}acetamido)- 3- methylpentanoate (L-Isoleucine methyl ester adduct, 7c)

Eluted with AcOEt/MeOH 9/1. **Yield:** 31%. White solid. **Mp:** 163-165 °C. **¹H -NMR** (400 MHz CDCl₃): δ (ppm) 8.04 (m, 2H), 7.60 (s, 1H), 7.51 (m, 5H), 7.34 (d, 2H, *J* = 7.6 Hz), 7.18 (d, 1H, *J* = 8.4 Hz), 4.50 (m, 1H), 4.06 (q, 2H, *J* = 15.6 Hz), 3.52 (s, 3H), 2.43 (s, 3H), 1.67 (m, 2H), 1.13 (m, 1H), 0.65 (m, 6H). **¹³C-NMR** (100 MHz CDCl₃): δ (ppm) 171.66, 167.78, 161.64, 158.96, 154.89, 140.66, 136.73, 132.82, 130.78, 129.76, 129.04, 128.22, 127.40, 116.50, 115.37, 103.37, 56.68, 51.79, 37.51, 33.88, 24.83, 21.30, 15.07, 11.23. **LRMS (ESI)** *m/z* = 488.0 [M+H]⁺ ; 510.0 [M+Na]⁺; 526.0 [M+K]⁺. **IR** (KBr) cm⁻¹: 3369 (NHCO), 2215 (CN), 1732 (CO ester), 1657 (CO amide). **Anal. calcd.** for C₂₈H₂₉N₃O₃S: C 68.97, H 5.99, N 8.62, S 6.58; **found:** C 68.75, H 5.97, N 8.72, S 6.43.

Methyl (2S)- 2- (2- {[3- cyano- 4- (4- methylphenyl)- 6- phenylpyridin- 2- yl]sulfanyl}acetamido)- 3- (1H- imidazol- 4- yl) propanoate (L-Histidine methyl ester adduct, 7d)

Eluted with AcOEt/MeOH 9/1. **Yield:** 30%. White solid. **Mp:** 135-141 °C. **¹H -NMR** (400 MHz CDCl₃): δ (ppm) 8.07 (m, 2H), 7.94 (d, 1H, *J* = 7.2 Hz), 7.57 (s, 1H), 7.52 (m, 5H), 7.39 (s, 1H), 7.34 (d, 2H, *J* = 8.0 Hz), 6.62 (s, 1H), 4.80 (m, 1H), 4.11 (s, 2H), 3.54 (s, 3H), 2.89-3.02 (2q, 2H, *J* = 15.0 Hz), 2.44 (s, 3H), 1.50 (m, 1H). **¹³C-NMR** (100 MHz CDCl₃): δ (ppm) 171.42, 167.99, 161.54, 158.70, 154.80, 140.08, 140.04, 136.77, 133.10, 132.96, 130.74, 129.76, 129.02, 128.21, 127.42, 116.33, 115.62, 99.42, 90.97, 52.32, 52.21, 45.20, 29.04, 21.28. **LRMS (ESI)** *m/z* = 512.0 [M+H]⁺ ; **IR** (KBr) cm⁻¹: 3361 (NH), 2221 (CN), 1741 (CO ester), 1654 (CO amide). **Anal. calcd.** for C₂₈H₂₅N₅O₃S: C 65.74, H 4.93, N 13.69, S 6.27; **found:** C 65.41, H 4.70, N 14.07, S 6.44.

Methyl (2S)- 3- carbamoyl- 2- (2- {[3- cyano- 4- (4- methylphenyl)- 6- phenylpyridin- 2- yl]sulfanyl}acetamido) propanoate (L-Arginine methyl ester adduct, 7e)

Eluted with DCM/MeOH 9/1. **Yield:** 27%. White solid. **Mp:** 161-171 °C. **¹H -NMR** (400 MHz CD₃OD): δ (ppm) 8.19 (m, 2H), 7.74 (s, 1H), 7.57 (d, 2H, *J* = 8.0 Hz), 7.50 (m, 3H), 7.37 (d, 2H, *J* = 8.0 Hz), 4.45 (m, 1H), 4.22 (q, 2H, *J* = 16.0 Hz), 3.59 (s, 3H), 3.02 (m, 2H), 2.43 (s, 3H), 1.62 (m, 1H), 1.82 (m, 1H), 1.47 (m, 2H). **¹³C-NMR** (100 MHz CD₃OD): 171.90, 169.20, 161.91, 158.74, 154.86, 140.40, 136.90, 133.01, 132.02, 130.40, 129.30, 129.25, 128.71, 128.17, 127.49, 126.60, 115.13, 48.16, 47.94, 47.09, 46.87, 40.29, 29.01,

24.59. **LRMS (ESI)** $m/z = 531.0 [M+H]^+ ; 553.0 [M+Na]^+$. **IR** (KBr) cm^{-1} : 3364 (NH), 2225 (CN), 1744 (CO ester), 1653 (CO amide). **Anal. calcd.** for $C_{28}H_{30}N_6O_3S$: C 63.38, H 5.70, N 15.84, S 6.04; **found**: C 63.44, H 5.44, N 15.75, S 6.42.

Methyl (2S)- 2- (2- {[3- cyano- 4- (4- methylphenyl)- 6- phenylpyridin- 2- yl]sulfanyl}acetamido)- 3- phenylpropanoate (L-Phenylalanine methyl ester adduct, 7f)

Eluted with AcOEt/MeOH 9/1. **Yield**: 34%. White solid. **Mp**: 167-173 °C. **1H -NMR** (400 MHz DMSO D_6): δ (ppm) 8.65 (d, 1H, $J = 7.6$ Hz), 8.25 (m, 2H), 7.87 (s, 1H), 7.64 (d, 2H, $J = 7.6$ Hz), 7.51 (m, 3H), 7.39 (d, 2H, $J = 7.6$ Hz), 7.12 (m, 5H), 4.47 (m, 1H), 4.14 (s, 2H), 3.49 (s, 3H), 2.85-2.99 (2q, 2H, $J = 14.0$ Hz), 2.40 (s, 3H). **^{13}C -NMR** (100 MHz DMSO D_6): δ (ppm) 171.37, 167.67, 161.43, 158.77, 154.73, 140.71, 136.60, 135.43, 132.88, 130.80, 129.84, 129.06, 128.71, 128.52, 128.21, 127.35, 126.80, 116.37, 115.32, 103.54, 53.15, 52.12, 37.52, 33.38, 24.04. **LRMS (ESI)** $m/z = 552.0 [M+H]^+ ; 544.0 [M+Na]^+ ; 560.0 [M+K]^+$. **IR** (KBr) cm^{-1} : 3300 (NHCO), 2217 (CN), 1742 (CO ester), 1655 (CO amide). **Anal. calcd.** for $C_{31}H_{27}N_3O_3S$: C 71.38, H 5.22, N 8.06, S 6.15; **found**: C 71.21, H 5.30, N 8.11, S 5.78.

Methyl (2S)- 2- (2- {[3- cyano- 4- (4- methylphenyl)- 6- phenylpyridin- 2- yl]sulfanyl}acetamido)- 3- (4- methoxyphenyl) propanoate (L-Tyrosine methyl ester adduct, 7g)

Eluted with Hexane/AcOEt 6/4. **Yield**: 21%. White solid. **Mp**: 215-217 °C. **1H -NMR** (400 MHz $CDCl_3$): δ (ppm) 8.03 (m, 2H), 7.58 (d, 2H, $J = 8$ Hz), 7.50 (m, 3H), 7.36 (d, 2H, $J = 7.6$ Hz), 7.25 (s, 1H), 7.10 (d, 1H, $J = 8.0$ Hz), 6.68 (d, 2H, $J = 8.2$ Hz), 6.45 (d, 2H, $J = 8.2$ Hz), 5.12 (bs, 1H), 4.77 (m, 1H), 3.99 (q, 2H, $J = 15.6$ Hz), 3.57 (s, 3H), 2.75-2.94 (2q, 2H, $J = 14.0$ Hz), 2.45 (s, 3H). **^{13}C -NMR** (400 MHz $CDCl_3$): δ (ppm) 171.47, 167.80, 161.42, 158.90, 154.81, 144.96, 140.69, 136.59, 132.84, 130.94, 129.79, 129.12, 129.02, 128.39, 127.57, 127.15, 116.56, 116.10, 115.40, 103.46, 53.17, 49.84, 36.58, 31.31, 21.29. **LRMS (ESI)** $m/z = 538.0 [M+H]^+ ; 540.6 [M+Na]^+$. **IR** (KBr) cm^{-1} : 3400-3200 (OH), 3306 (NH), 2218 (CN), 1730 (CO ester), 1656 (CO amide). **Anal. calcd.** for $C_{31}H_{27}N_3O_4S$: C 69.25, H 5.06, N 7.82, S 5.96; **found**: C 69.61, H 5.32, N 7.99, S 5.83.

1,5- Dimethyl (2S)- 2- (2- {[3- cyano- 4- (4- methylphenyl)- 6- phenylpyridin- 2- yl]sulfanyl}acetamido) pentanedioate (L-Glutammate methyl diester adduct, 7h)

Eluted with Hexane/AcOEt 1/1. **Yield**: 27%. White solid. **Mp**: 179-193 °C. **1H -NMR** (400 MHz $CDCl_3$): δ (ppm) 8.06 (m, 2H), 7.61 (s, 1H), 7.54 (d, 2H, $J = 7.6$ Hz), 7.50 (m, 3H), 7.35 (d, 2H, $J = 7.6$ Hz), 7.25 (s, 1H), 4.58 (m, 1H), 4.05 (q, 2H, $J = 15.8$ Hz), 3.55 (s, 3H), 3.54 (s, 3H), 2.44 (s, 3H), 2.09 (m, 2H), 1.78 (m, 2H). **^{13}C -NMR** (400 MHz $CDCl_3$): δ (ppm) 171.30, 168.01, 162.70, 161.80, 158.97, 155.00, 140.66, 136.66, 132.85, 130.80, 129.78, 129.11, 128.29, 127.47, 116.61, 115.37, 103.86, 59.91, 59.12, 53.05, 52.20, 41.80, 37.02, 20.50. **LRMS (ESI)** $m/z = 518.0 [M+H]^+ ; 540.0 [M+Na]^+ ; 556.0 [M+K]^+$. **IR** (KBr) cm^{-1} : 3312 (NHCO), 2215 (CN), 1732 (CO ester), 1653 (CO amide). **Anal. calcd.** for $C_{28}H_{27}N_3O_5S$: C 64.97, H 5.26, N 8.12, S 6.20; **found**: C 65.01, H 5.43, N 8.49, S 6.06.

(2S)- 2- (2- {[3- Cyano- 4- (4- methylphenyl)- 6- phenylpyridin- 2- yl]sulfanyl}acetamido)- 3- methylbutanoic acid (L-Valine free acid adduct, 8)

To a stirred solution of **7a** (24 mg, 0.05 mmol) in a 3/1/0.5 mixture of THF/EtOH/H₂O (2 mL), NaOH 1 N (0.22 mL, 0.22 mmol) was added. The mixture was stirred at room temperature for 15 min until the solution becomes yellow. The reaction was quenched with HCl 2 N and extracted with AcOEt. The organic phase was washed with water, dried over Na₂SO₄, filtered and concentrated under reduced pressure. The crude residue was purified through flash chromatography on silica gel, eluting with AcOEt/MeOH/AcOH 9/1/0.5 to give pure **8**. **TLC R_f** (DCM/MeOH 9/1) 0.61. **Yield:** 40%. **¹H-NMR** (400 MHz CD₃OD): δ (ppm) 8.19 (d, 2H, *J* = 8.0 Hz), 7.76 (s, 1H), 7.58 (d, 2H, *J* = 8.0 Hz), 7.50 (m, 3H), 7.38 (d, 2H, *J* = 8.0 Hz), 4.24 (d, 1H, *J* = 16.0 Hz), 4.17 (q, 2H, *J* = 16.0 Hz), 2.44 (s, 3H), 2.06 (m, 1H), 0.74 (d, 3H, *J* = 16.0 Hz), 0.73 (d, 3H, *J* = 16.0 Hz). **¹³C-NMR** (100 MHz CD₃OD): δ (ppm) 174.15, 171.31, 162.55, 158.39, 154.47, 140.11, 137.09, 133.22, 131.31, 129.74, 129.31, 128.80, 128.15, 116.41, 116.21, 102.78, 31.10, 30.40, 23.40, 21.30, 18.99. **LRMS (ESI)** *m/z* = 459.8 [M+H]⁺; 481.8 [M+Na]⁺. **IR** (KBr) cm⁻¹: 3450-3100 (OH), 3362 (NHCO), 2221 (CN), 1690 (CO acid), 1646 (CO amide). **Anal. calcd.** for C₂₆H₂₅N₃O₃S: C 67.95, H 5.48, N 9.14, S 6.98; **found:** C 68.02, H 5.33, N 8.96, S 6.79.

2.3. Synthetic procedure for diamino acid adducts (9 and 10)

1,4- Dimethyl(2S)- 2- [(2S)- 2- ([(9H- fluoren- 9- yl)methoxy]carbonyl)amino)- 3- methylbutanamido] butanedioate (Fmoc-Val-Asp-OMe(OMe), 16)

Same amidation protocol used for **7a-h**: To a stirring solution of Fmoc-Valine (500 mg, 1.47 mmol) in dry DMF (5 mL) a solution of L-aspartate dimethyl ester (hydrochloride salt; 291 mg, 1.47 mmol) in dry DMF (53 mL) was added dropwise at 0 °C under N₂ atmosphere. Then EDC (282 mg, 1.47 mmol), HOBt (199 mg, 1.47 mmol) and dry DIPEA (0.31 mL, 1.77 mmol) were added. The mixture was stirred 30 min at 0 °C and then 4 h at room temperature. The reaction was quenched with water and then it was extracted with AcOEt. The organic phase was washed with water, dried over Na₂SO₄, filtered and concentrated under reduced pressure. The crude residue was purified through flash chromatography on silica gel. Eluted with Hexane/AcOEt 1/1. **TLC R_f** (Hexane/AcOEt 1/1) 0.55. **Yield:** 79%. **¹H-NMR** (400 MHz CDCl₃): δ (ppm) 7.74 (d, 2H, *J* = 8.0 Hz), 7.58 (d, 2H, *J* = 6.4 Hz), 7.38 (t, 2H, *J* = 7.2 Hz), 7.29 (t, 2H, *J* = 7.2 Hz), 6.92 (d, 1H, *J* = 7.6 Hz), 5.56 (d, 1H, *J* = 8.4), 4.89 (m, 1H), 4.37 (m, 2H), 4.21 (t, 1H, *J* = 6.8 Hz), 4.10 (m, 1H), 3.73 (s, 3H), 3.66 (s, 3H), 3.04 (dd, 1H, *J* = 13.6 Hz), 2.83 (dd, 1H, *J* = 4.4 Hz, *J* = 17.2 Hz), 2.13 (m, 1H), 0.99 (d, 3H, *J* = 6.0 Hz), 0.96 (d, 3H, *J* = 6.0 Hz). **¹³C-NMR** (100 MHz CDCl₃) δ (ppm) 171.08, 170.70, 156.23, 143.71, 141.21, 127.62, 126.99, 125.08, 119.79, 67.10, 60.06, 52.68, 52.04, 48.32, 47.06, 35.80, 31.44, 18.88, 17.62. **LRMS (ESI)** *m/z* = 483.0 [M+H]⁺; 505.2 [M+Na]⁺. **IR** (KBr) cm⁻¹: 3362 (NHCO), 1745 (CO ester), 1649 (CO amide). **Anal. calcd.** for C₂₆H₃₀N₂O₇: C 64.72, H 6.27, N 5.81; **found:** C 64.51, H 6.25, N 6.09.

1,4- Dimethyl (2S)- 2- [(2S)- 2- amino- 3- methylbutanamido]butanedioate (NH₂-Val-Asp-OMe(OMe), 17)

To a stirred solution of **16** (271 mg, 0.56 mmol) in DMF (7 mL), NaN₃ (73 mg, 1.12 mmol) was added. The mixture was stirred at 50 °C for 12 h. The reaction was quenched with water and extracted with AcOEt. The organic phase was washed with water, dried over Na₂SO₄, filtered and concentrated under reduced pressure. The crude residue was used in the next step without further purification. **TLC R_f** (Hexane/AcOEt 3/1) 0.57. **LRMS (ESI) m/z** = 261.8 [M+H]⁺.

1,4- Dimethyl (2S)- 2- [(2S)- 2- (2- {[3- cyano- 4- (4- methylphenyl)- 6- phenylpyridin- 2- yl]sulfanyl} acetamido)- 3- methylbutanamido]butanedioate (Diamino acid methyl diester adduct, 9)

Same amidation protocol used for **7a-h**: To the crude of **17a**, dry DMF (3 mL) was added under N₂ atmosphere. Then a solution of **15** (112 mg, 0.31 mmol) in dry DMF (3 mL) was added dropwise at 0 °C. EDC (42 mg, 0.31 mmol), HOBt (59 mg, 0.31 mmol) and dry DIPEA (0.06 mL, 0.37 mmol) were added. The mixture was stirred 30 min at 0 °C and then 12 h at room temperature. The reaction was quenched with water and then it was extracted with AcOEt. The organic phase was washed with water, dried over Na₂SO₄, filtered and concentrated under reduced pressure. The crude residue was purified through flash chromatography on silica gel. Eluted with AcOEt. **TLC R_f** (AcOEt) 0.56. **Yield:** (over two steps): 21%. **¹H NMR** (400 MHz CDCl₃): δ (ppm) 8.04 (d, 2H, *J* = 6.0 Hz), 7.58 (s, 1H), 7.53 (m, 2H), 7.48 (m, 3H), 7.30 (m, 2H), 6.79 (d, 1H, *J* = 8.0 Hz), 4.73 (m, 1H), 4.25 (t, 1H, *J* = 7.2 Hz), 4.16 (d, 1H, *J* = 15.6 Hz), 4.00 (d, 2H, *J* = 15.6 Hz), 3.69 (s, 3H), 3.64 (s, 3H), 2.91 (dd, 1H, *J* = 17.2 Hz), 2.62 (dd, 1H, *J* = 4.4 Hz, *J* = 17.2 Hz), 2.43 (s, 3H), 1.93 (m, 1H), 0.75 (d, 3H, *J* = 6.8 Hz), 0.67 (d, 3H, *J* = 6.8 Hz). **¹³C-NMR** (100 MHz CDCl₃): δ (ppm) 171.08, 170.70, 156.23, 143.85, 130.73, 129.97, 129.76, 129.04, 128.23, 127.40, 116.58, 115.37, 79.41, 58.60, 52.67, 52.02, 48.15, 35.65, 31.82, 29.59, 29.24, 26.30, 22.58, 21.28, 18.66, 17.54, 14.01. **LRMS (ESI) m/z** = 602.8 [M+H]⁺; 624.8 [M+Na]⁺. **IR** (KBr) cm⁻¹: 3361 (NHCO), 2225 (CN), 1742 (CO ester), 1651 (CO amide). **Anal. calcd.** for C₃₂H₃₄N₄O₆S: C 63.77, H 5.69, N 9.30, S 5.32; **found:** C 63.81, H 5.75, N 9.09, S 5.64

(2S)- 2- [(2S)- 2- (2- {[3- Cyano- 4- (4- methylphenyl)- 6- phenylpyridin- 2- yl]sulfanyl}acetamido)- 3- methylbutanamido]butanedioic acid (Diamino acid acid free adduct, 10)

To a stirred solution of **9** (34 mg, 0.05 mmol) in a 3/1/0.5 mixture of THF/EtOH/H₂O (2 mL), NaOH 1 N (0.22 mL, 0.22 mmol) was added. The mixture was stirred at room temperature for 15 min until the solution becomes yellow. The reaction was quenched with HCl 2 N and extracted with AcOEt. The organic phase was washed with water, dried over Na₂SO₄, filtered and concentrated under reduced pressure. The crude residue was purified through flash chromatography on silica gel, eluting with AcOEt/MeOH/AcOH 9/1/0.5 to give pure **10**. **TLC R_f** (AcOEt) 0.41. **Yield:** 61%. **¹H-NMR** (400 MHz CD₃OD): δ (ppm) 8.04 (d, 2H, *J* = 6.8Hz), 7.56 (s, 1H), 7.54 (m, 3H), 7.40 (m, 4H), 4.65 (t, 1H, *J* = 5.6 Hz), 4.41 (m, 1H), 3.83 (m, 1H), 3.16 (m, 1H), 2.20 (m, 2H), 1.02 (d, 3H, *J* = 7.2 Hz), 1.01 (d, 3H, *J* = 7.2 Hz). **¹³C-NMR** (100 MHz CD₃OD): δ (ppm) 173.08, 171.90, 165.58; 160.06, 156.68, 148.15, 145.94, 139.17, 137.92; 129.29; 128.42; 128.23; 127.72; 126.88; 121.38; 118.27, 98.30, 63.48, 58.54, 49.71, 36.71, 30.82, 29.25, 19.87, 18.39, 17.39. **LRMS (ESI) m/z** = 574.9 [M+H]⁺; 573.0 [M-H]. **IR** (KBr) cm⁻¹: 3420-3090 (OH), 3361 (NHCO), 2225 (CN), 1688 (CO acid), 1640

(CO amide). **Anal. calcd.** for C₃₀H₃₀N₄O₆S: C 62.70, H 5.26, N 9.75, S 5.58; **found:** C 62.80, H 5.35, N 9.89, S 5.62.

2.4. Synthetic procedure for triamino acid adduct (11)

(2S)- 2- [(2S)- 3 Carboxy- 2- [(2S)- 2- ([(9H- fluoren- 9- yl)methoxy]carbonyl)amino)- 3-methylbutanamido] propanamido]- 4- (methylsulfanyl)butanoic acid (Resin-free Fmoc-tripeptide, 19)

Resin-bounded compound **18** was charged in a gooch filter and treated with a 88/2/5/5 cleavage solution of TFA/TIPS/H₂O/DTT (20 mL) under an upward flux of N₂. After 1 h the resin was filtered and the filtrate was recovered and evaporated under reduced pressure. The white solid obtained was washed with hexane and toluene and used directly in the next step.

Resin-bounded tripeptide (18)

Compound **18** has been obtained by MW-SPPS (microwave solid phase peptide synthesis) using an MW automated CEM Peptide Synthesizer. The instrument has been charged with Fmoc-methionine on Wang resin (167 mg) previously swallowed in DMF through a fritted buchner funnel under N₂ flux for 2 h. The instrument was also charged with: Fmoc-Val-OH (2N, 408 mg in 6 mL of DMF); Fmoc- Asp(OtBu)-OH (2N, 492 mg in 6 mL of DMF); a HOBt and HBTU (270 mg and 758 mg respectively in 4 mL of DMF); DIPEA (2 mL of 34.8 % v/v DMF); piperidine (100 mL of 20% v/v DMF); DCM (2 L); DMF (2 L). Then the instrument was set and the synthetic procedure lasted for 3 h and 37 min. The obtained resin was removed from the instrument and washed several times with DMF and DCM.

Methyl (2S)- 2- [(2S)- 2- [(2S)- 2- ([(9H- fluoren- 9- yl)methoxy]carbonyl)amino)- 3-methylbutanamido]- 4- methoxy- 4- oxobutanamido]- 4- (methylsulfanyl)butanoate (methyl diester Fmoc-tripeptide, 20)

To a stirred solution of **19** (170 mg, 0.29 mmol) in dry MeOH (10 mL), freshly distilled SOCl₂ (0.22 mL, 2.90 mmol) was added at 0 °C. The mixture was stirred at 0 °C for 30 min and then at room temperature for 6 h. Solvent was removed under reduced pressure. The crude residue was purified through flash chromatography on silica gel, eluting with AcOEt to give **20**. **TLC R_f** (AcOEt) 0.69. **Yield:** 28%. **¹H-NMR** (400 MHz CDCl₃): δ (ppm) 7.75 (d, 2H, *J* = 7.6 Hz), 7.58 (d, 2H, *J* = 7.2 Hz), 7.39 (t, 2H, *J* = 7.6 Hz), 7.31 (t, 2H, *J* = 7.6 Hz), 5.40 (m, 1H), 4.82 (m, 1H), 4.62 (m, 1H), 4.44 (m, 2H), 4.23 (t, 1H, *J* = 6.8 Hz), 4.00 (m, 1H), 3.72 (s, 3H), 3.68 (s, 3H), 3.04 (m, 1H), 2.99 (m, 1H), 2.67 (t, 2H, *J* = 6.4 Hz), 2.53 (m, 2H), 2.16 (s, 3H), 1.99 (m, 1H), 0.98 (d, 3H), 0.95 (d, 3H). **¹³C-NMR** (100 MHz DMSO): δ (ppm) 172.91, 170.70, 170.31, 156.23, 143.71, 141.21, 127.62, 126.99, 125.08, 119.98, 119.79, 67.10, 65.69, 60.06, 55.11, 52.04, 51.89, 48.32, 47.06, 35.80, 31.44, 31.00, 27.91, 18.88, 17.62, 15.47. **LRMS (ESI)** *m/z* = 613.7 [M+H]⁺; 636.7 [M+ Na]⁺; 652.0 [M+ K]⁺. **IR** (KBr) cm⁻¹: 3361 (NHCO), 1742 (CO ester), 1651 (CO amide). **Anal. calcd.** for C₃₁H₃₉N₃O₈S: C 60.67, H 6.41, N 6.85, S 5.22; **found:** C 60.42, H 6.35, N 7.09, S 5.44.

Methyl (2S)- 2- [(2S)- 2- [(2S)- 2- amino- 3- methylbutanamido]- 4- methoxy- 4- oxobutanamido]- 4- (methylsulfanyl) butanoate (Free amine tripeptide, 21)

Same deprotection protocol used for **17**. To a stirred solution of **20** (48 mg, 0.79 mmol) in DMF (a mL), NaN₃ (13 mg, 0.20 mmol) was added. The mixture was stirred at 50 °C for 4 h. The reaction was quenched with water and extracted with AcOEt. The organic phase was washed with water, dried over Na₂SO₄, filtered and concentrated under reduced pressure. The crude residue was purified through flash chromatography on silica gel, eluting with AcOEt/MeOH 9/1 to give **21**. **TLC R_f** (AcOEt) 0.47. **Yield:** 62%. **LRMS (ESI)** m/z = 391.8 [M+H]⁺; 414.0 [M+ Na]⁺; 430.1 [M+ K]⁺. **IR** (KBr) cm⁻¹: 3401 (NH), 3361 (NHCO), 1742 (CO ester), 1651 (CO amide). **Anal. calcd.** for C₁₆H₂₉N₃O₆S: C 49.09, H 7.47, N 10.73, S 8.19; **found:** C 49.24, H 7.38, N 10.89, S 8.44.

Methyl (2S)- 2- [(2S)- 2- [(2S)- 2- (2- {[3- cyano- 4- (4- methylphenyl)- 6- phenylpyridin- 2- yl]sulfanyl} acetamido)- 3- methylbutanamido]- 4- methoxy- 4- oxobutanamido]- 4- (methylsulfanyl)butanoate (Tripeptide methyl diester adduct, 11)

Same amidation protocol used for **7a-h**. To a stirring solution of **21** (7 mg, 0.02 mmol) in dry DMF (1 mL) a solution of **15** (6 mg, 0.02 mmol) in dry DMF (0.5 mL) was added dropwise at 0 °C under N₂ atmosphere. Then EDC (3 mg, 0.02 mmol), HOBt (2 mg, 0.02 mmol) and dry DIPEA (0.01 mL, 0.02 mmol) were added. The mixture was stirred 30 min at 0 °C and then 12 h at room temperature. The reaction was quenched with water and then extracted with AcOEt. The organic phase was washed with water, dried over Na₂SO₄, filtered and concentrated under reduced pressure. The crude residue was purified through flash chromatography on silica gel, eluting with AcOEt to give **11**. **Yield:** 41%. **¹H-NMR** (400 MHz CD₃OD): δ (ppm) 8.19 (d, 2H, *J* = 2.4 Hz), 7.77 (s, 1H), 7.60 (d, 2H, *J* = 8.0 Hz), 7.51 (m, 3H), 7.38 (d, 2H, *J* = 8.0 Hz), 4.94 (m, 1H), 4.52 (m, 1H), 4.43 (m, 1H), 3.70 (m, 2H), 3.30 (s, 6H), 2.94 (d, 1H, *J* = 8.0 Hz), 2.90 (d, 1H, *J* = 8.0 Hz), 2.54 (m, 2H), 2.53 (m, 1H), 2.44 (s, 3H), 2.29 (m, 2H), 2.00 (s, 3H), 0.81 (d, 3H, *J* = 6.8 Hz), 0.76 (d, 3H, *J* = 76.8 Hz). **¹³C-NMR** (100 MHz DMSO): δ (ppm) 172.09, 171.65, 156.25, 143.70, 130.69, 129.97, 129.76, 129.04, 128.25, 127.50, 116.45, 115.37, 79.41, 58.60, 55.10, 52.00, 48.15, 35.65, 31.82, 31.09, 29.59, 29.31, 29.24, 26.30, 23.33, 22.49, 21.28, 18.66, 17.54, 15.13, 14.01. **IR** (KBr) cm⁻¹: 3369 (NHCO), 2218 (CN), 1749 (CO ester), 1647 (CO amide). **Anal. calcd.** for C₃₇H₄₃N₅O₇S₂: C 60.55, H 5.91, N 9.54, S 8.74; **found:** C 60.41, H 6.15, N 9.59, S 8.84.

***Tert*-butyl (hydroxymethyl)carbamate (22)**

t-butoxy carbamide (300 mg, 2.56 mmol), water (2 mL), formaldehyde (37% in H₂O, 0.52 mL, 6.41 mmol) and K₂CO₃ (7 mg, 0.05 mmol) were charged into a round bottomed flask with a magnetic stirrer. The mixture was heated to 65 °C and stirred for 1 h. After cooling the mixture was extracted with AcOEt. The organic phase was washed with water, dried over Na₂SO₄, filtered and concentrated under reduced pressure. The crude residue was purified through flash chromatography on silica gel, eluting with Hexane/AcOEt 3/2 to give compound **23b** as white solid. **Yield:** 42%. **¹H-NMR** (400 MHz CDCl₃): δ (ppm) 5.93 (s, 1H), 4.59 (s, 2H), 4.39 (s, 1H), 1.39 (s, 9H). **¹³C-NMR** (100 MHz CDCl₃): δ (ppm) 156.07, 80.02, 65.41, 28.19. **LRMS (ESI)**

$m/z = 169.9$ $[M+Na]^+$. **IR** (KBr) cm^{-1} : 3402-3195 (OH), 3360 (NHCO), 1755 (CO ester), 1640 (CO amide). **Anal. calcd.** for $C_6H_{13}NO_3$: C 48.97, H 8.90, N 9.52; **found**: C 48.84, H 8.85, N 9.44.

***Tert*-butyl (((3-cyano-6-phenyl-4-(*p*-tolyl)pyridin-2-yl)thio)methyl)carbamate (23)**

To a stirred solution of compound **23** (80 mg, 0.54 mmol) in DCM (1 mL), triphenylphosphine (PPh_3) (214 mg, 0.81 mmol) was added. The mixture was cooled in an ice-bath and CBr_4 (334 mg, 1.09 mmol) was added. The mixture was irradiated with MW for 15 min at 40 °C. The solution obtained was added dropwise to **14** (82 mg, 0.27 mmol) and trimethylamine (0.07 mL, 0.54 mmol) in DCM (2 mL). The mixture was stirred at room temperature for 12 h. The reaction was quenched with water and extracted with DCM. The organic phase was washed with water, dried over Na_2SO_4 , filtered and concentrated under reduced pressure. The crude residue was purified through flash chromatography on silica gel, eluting with Hexane/AcOEt 9/1 give compound **23**. **Yield**: 49%. **¹H-NMR** (400 MHz $CDCl_3$): δ (ppm) 8.03 (m, 2H), 7.55 (s, 1H), 7.52 (m, 5H), 7.39 (d, 2H, $J = 8.0$ Hz), 5.77 (s, 1H), 5.11 (d, 2H, $J = 4.0$ Hz), 2.43 (s, 3H), 1.49 (s, 9H). **LRMS (ESI)** $m/z = 432.8$ $[M+H]^+$. **IR** (KBr) cm^{-1} : 3360 (NHCO), 2218 (CN), 1755 (CO ester), 1640 (CO amide). **Anal. calcd.** for $C_{25}H_{25}N_3O_2S$: C 69.58, H 5.84, N 9.74, S 7.43; **found**: C 69.60, H 5.95, N 9.81, S 7.74.

2-((3-cyano-6-phenyl-4-(*p*-tolyl)pyridin-2-yl)thio)acetamide (24)

To a stirred solution of 2-mercapto-pyridine **14** (120 mg, 0.40 mmol) in DMF (2 mL) a 10% aqueous solution of KOH (0.15 mL, 0.27 mmol) was added and the mixture was stirred at room temperature for 30 min. The mixture becomes red and then a solution of 2-Bromoacetamide (60 mg, 0.40 mmol) in DMF (0.5 mL) was added dropwise. The mixture was stirred for further 3h at room temperature. The reaction was treated with HCl 1 N and extracted with AcOEt. The organic phase was washed with water, dried over Na_2SO_4 , filtered and concentrated under reduced pressure. The crude residue was purified through flash chromatography on silica gel, eluting with Hexane/AcOEt 1/1 to give compound **24** as pale yellow solid. **Yield**: 50%. **¹H-NMR** (400 MHz $CDCl_3$): δ (ppm) 8.08 (d, 2H, $J = 8.0$ Hz), 7.50 (s, 1H), 7.48-7.44 (m, 3H), 7.38-7.31 (m, 4H), 5.96 (bs, 2H), 5.70 (s, 2H), 2.45 (s, 3H). **¹³C-NMR** (100 MHz $CDCl_3$): δ (ppm) 170.54, 162.50, 158.40, 154.56, 140.47, 137.01, 133.11, 131.16, 129.66, 129.25, 128.97, 128.05, 116.44, 116.12, 102.42, 33.37, 21.27. **LRMS (ESI)** $m/z = 359.8$ $[M+H]^+$; 381.8 $[M+Na]^+$. **IR** (KBr) cm^{-1} : 3300 (NHCO), 2218 (CN) 1644 (CO amide). **Anal. calcd.** for $C_{21}H_{17}N_3OS$: C 70.17, H 4.77, N 11.69, S 8.92; **found**: C 69.98, H 4.95, N 11.77, S 8.74.

3. BIOLOGY SECTION

Cells and Virus. Human embryonic kidney 293T (HEK 293T) and Madin–Darby canine kidney (MDCK) cells were cultivated in Dulbecco’s modified Eagle’s medium (DMEM, Life Technologies) supplemented with 10% (v/v) fetal bovine serum (FBS, Life Technologies) and antibiotics (100 U/mL penicillin and 100 μ g/mL streptomycin, Life Technologies). The cells were maintained at 37 °C in a 5% CO_2 humidified atmosphere. Influenza A/PR/8/34 virus (PR8 strain, H1N1, Cambridge lineage) was obtained from P. Digard (Roslin Institute, University of Edinburgh, United Kingdom).

Compounds and Peptide. Ribavirin (RBV; 1-D-ribofuranosyl-1,2,4-triazole-3-carboxamide) and oseltamivir carboxylic acid (OSV), the active form of oseltamivir [(3R,4R,5S)-4-acetamido-5-amino-3-(1-ethylpropoxy)-

1-cyclohexene-1-carboxylic acid] were obtained from Roche. The PB1₁₋₁₅-Tat peptide was synthesized and purified by the Peptide Facility of CRIBI Biotechnology Center (University of Padua, Padua, Italy). The PB1₁₋₁₅-Tat peptide possesses a C-terminal sequence from the HIV Tat protein (amino acids 47–59) to mediate cell entry.

PA–PB1 Interaction Enzyme-Linked Immunosorbent Assay (ELISA). The PA–PB1 interaction was detected as described by Trist et al.[71] Briefly, microtiter plates (Nuova Aptca) were incubated with 400 ng of 6His-PA_(239–716) for 3 h at 37 °C and then blocked with 2% BSA (Sigma) in PBS for 1 h at 37 °C. After washing, 200 ng of GST-PB1_(1–25) or GST as a control, dissolved in serum-free DMEM, in the presence of test compounds at various concentrations or DMSO, were added and incubated overnight at room temperature. *E. coli*-expressed, purified 6His-PA_(239–716), GST, and GST-PB1_(1–25) proteins were obtained as previously described.[50,88] After washing, the interaction between 6His-PA_(239–716) and GST-PB1_(1–25) was detected with an anti-GST monoclonal antibody conjugated to horseradish peroxidase (HRP; GenScript). After the final wash step, the substrate 3,3',5,5'-tetramethylbenzidine (TMB, KPL) was added, and the optical density was determined at 450 nm by an ELISA plate reader (Tecan Sunrise). Values obtained from the samples treated with only DMSO were used to set as 100% of PA–PB1 interaction. The PB1_(1–15)-Tat peptide was included in all experiments as positive control for inhibition.

Plaque Reduction Assay (PRA). Antiviral activity of compounds was investigated using PRAs, as described elsewhere.[89] Briefly, a confluent monolayer of MDCK cells was seeded in 12-well plates. Cells were infected with FluA virus (PR8 strain) at 40 PFU/well in DMEM supplemented with 1 µg/mL of TPCK-treated trypsin (Worthington Biochemical Corporation) and 0.14% BSA in the presence of various concentrations of test compounds for 1 h at 37 °C. Medium containing 1 µg/mL of TPCK-treated trypsin, 0.14% BSA, 1.2% Avicel, and test compounds at the same concentrations was then added. After 2 days of incubation, cell monolayers were fixed with 4% formaldehyde and stained with 0.1% toluidine blue, and viral plaques were counted. Ribavirin and oseltamivir carboxylic acid were included in all experiments as reference compounds. The mean plaque number obtained from the samples treated with DMSO was set at 100%.

Cytotoxicity Assay. Cytotoxicity of test compounds was assessed in MDCK and HEK 293T cells by the 3-(4,5-dimethylthiazol-2-yl)-2,5-diphenyltetrazolium bromide (MTT) method, as previously reported.[90,91] Briefly, MDCK cells (5×10^3 cells/well on 96-well plates) and HEK 293T (2×10^4 cells/well on 96-well plates) cells were incubated with test compounds at 2-fold serial dilutions from 250 µM or DMSO. After 24 or 48 h for HEK 293T and MDCK cells, respectively, MTT solution (5 mg/mL in PBS) was added to each well, and plates were incubated for 4 h at 37 °C. Then, a solubilization solution was added to lyse cells. After 3 h of further incubation at 37 °C, absorbance was read at 620 nm using an ELISA plate reader (Tecan Sunrise). Values obtained from the wells treated with only DMSO were used to set as 100% of viable cells.

Minireplicon Assay. HEK 293T cells were seeded at a density of 2×10^5 per well into 24-well plates. After 24 h, cells were transfected with pcDNA-PB1, pcDNA-PB2, pcDNA-PA, and pcDNA-NP plasmids (100 ng/well of each), expressing the Flu A/PR/8/34 virus PB1, PB2, PA, and NP proteins, respectively, along with pPolI-Flu-ffLuc plasmid (50 ng/well), containing an influenza virus-based luciferase minireplicon vRNA

under the control of the human RNA polymerase I promoter. Plasmids pcDNA-PB1, pcDNA-PB2, pcDNA-PA, and pcDNA-NP were generated as described elsewhere[92] and were kindly provided by P. Digard (Roslin Institute, University of Edinburgh, United Kingdom), whereas the plasmid pPolIFlu-ffLuc was provided by L. Tiley (University of Cambridge, United Kingdom). The transfection mixture also contained pRL-SV40 plasmid (50 ng/well, Promega), which constitutively expresses the *Renilla* luciferase, to normalize variations in transfection efficiency. Transfections were performed using calcium phosphate protocol in the presence of the test compounds or DMSO. Cell medium was replaced 4 h post-transfection with DMEM containing compounds or DMSO. At 24 h post-transfection, cells were harvested and both firefly luciferase and *Renilla* luciferase expression were determined using the Dual Luciferase Assay Kit from Promega. Ribavirin was included in all experiments as the reference compound.

Interference compound assessment. The behaviour of all the tested compounds (**7-11, 15, 23** and **24**) as PAINS (Pan-Assay Interference Compounds) [93] was examined through prediction by the online FAFDrugs4[94–96] (Free ADME-Tox Filtering Tool) program. Through its tool Bank-Formatter the compound library was prepared and then screened with the three different available filters A, B and C. All the analysed compounds resulted “accepted” by the software.[97]

ACKNOWLEDGMENTS

We thank P. Digard for providing plasmids and the Flu A A/PR/8/34 strain and L. Tiley for providing the plasmid pPolIFlu-ffLuc. This work was supported by Associazione Italiana per la Ricerca sul Cancro (AIRC, grant n. IG18855) and by the University of Padua (Progetto di Ricerca di Ateneo 2014, grant no. PDA141311) to A. Loregian.

Notes. The authors declare no competing financial interest.

REFERENCES

- [1] B.M. Hause, E.A. Collin, R. Liu, B. Huang, Z. Sheng, W. Lu, D. Wang, E.A. Nelson, F. Li, Characterization of a novel influenza virus in cattle and Swine: proposal for a new genus in the Orthomyxoviridae family., *MBio*. 5 (2014) e00031-14. doi:10.1128/mBio.00031-14.
- [2] L. Ferguson, A.K. Olivier, S. Genova, W.B. Epperson, D.R. Smith, L. Schneider, K. Barton, K. McCuan, R.J. Webby, X.-F. Wan, Pathogenesis of Influenza D Virus in Cattle., *J. Virol.* 90 (2016) 5636–42. doi:10.1128/JVI.03122-15.
- [3] R.B. Couch, Orthomyxoviruses, University of Texas Medical Branch at Galveston, 1996.
- [4] M.W. Report, Estimated Influenza Illnesses and Hospitalizations Averted by Influenza Vaccination — United States , 2012 – 13 Influenza Season, *62* (2013) 997–1000.
- [5] B. Cao, X. Li, Y. Mao, J. Wang, H. Lu, Y. Chen, Z. Liang, L. Liang, S. Zhang, B. Zhang, L. Gu, L. Lu, D. Wang, D. Ph, C. Wang, N. Influenza, *A.P.H.N. Clinical, new england journal*, (2009) 2507–2517.
- [6] E. Nobusawa, K. Sato, Comparison of the Mutation Rates of Human Influenza A and B Viruses, *80* (2006) 3675–3678. doi:10.1128/JVI.80.7.3675.

- [7] R. Chen, E.C. Holmes, Avian Influenza Virus Exhibits Rapid Evolutionary Dynamics, *Mol. Biol. Evol.* 23 (2006) 2336–2341. doi:10.1093/molbev/msl102.
- [8] M.D. Pauly, M.C. Procario, A.S. Lauring, A novel twelve class fluctuation test reveals higher than expected mutation rates for influenza A viruses, *Elife.* 6 (2017) e26437. doi:10.7554/eLife.26437.
- [9] R.-X. Gu, L.A. Liu, D.-Q. Wei, Structural and energetic analysis of drug inhibition of the influenza A M2 proton channel, *Trends Pharmacol. Sci.* 34 (2013) 571–580. doi:10.1016/J.TIPS.2013.08.003.
- [10] A. Moscona, Global Transmission of Oseltamivir-Resistant Influenza, *N. Engl. J. Med.* 360 (2009) 953–956. doi:10.1056/NEJMp0900648.
- [11] V.M. Deyde, X. Xu, R.A. Bright, M. Shaw, C.B. Smith, Y. Zhang, Y. Shu, L.V. Gubareva, N.J. Cox, A.I. Klimov, Surveillance of Resistance to Adamantanes among Influenza A(H3N2) and A(H1N1) Viruses Isolated Worldwide, *J. Infect. Dis.* 196 (2007) 249–257. doi:10.1086/518936.
- [12] S. Chutinimitkul, K. Suwannakarn, T. Chieochansin, L.Q. Mai, S. Damrongwatanapokin, A. Chaisingh, A. Amonsin, O. Landt, T. Songserm, A. Theamboonlers, Y. Poovorawan, H5N1 Oseltamivir-resistance detection by real-time PCR using two high sensitivity labeled TaqMan probes, *J. Virol. Methods.* 139 (2007) 44–49. doi:10.1016/j.jviromet.2006.09.007.
- [13] H. Zaraket, R. Saito, Y. Suzuki, T. Baranovich, C. Dapat, I. Caperig-Dapat, H. Suzuki, Genetic makeup of amantadine-resistant and oseltamivir-resistant human influenza A/H1N1 viruses., *J. Clin. Microbiol.* 48 (2010) 1085–92. doi:10.1128/JCM.01532-09.
- [14] H.K. Lee, C.K. Lee, T.P. Loh, J.W.-T. Tang, P.A. Tambyah, E.S.-C. Koay, High-Resolution Melting Approach to Efficient Identification and Quantification of H275Y Mutant Influenza H1N1/2009 Virus in Mixed-Virus-Population Samples, *J. Clin. Microbiol.* 49 (2011) 3555–3559. doi:10.1128/JCM.01087-11.
- [15] C. Thornsberry, Regional trends in antimicrobial resistance among clinical isolates of *Streptococcus pneumoniae*, *Haemophilus influenzae*, and *Moraxella catarrhalis* in the United States: results from the TRUST Surveillance Program, 1999-2000, *Clin. Infect. Dis.* 34 (2002) S4–S16. <http://dx.doi.org/10.1086/324525>.
- [16] R.A. Bright, D.K. Shay, B. Shu, N.J. Cox, A.I. Klimov, Adamantane Resistance Among Influenza A Viruses Isolated Early During the 2005-2006 Influenza Season in the United States, *JAMA.* 295 (2006) 891. doi:10.1001/jama.295.8.joc60020.
- [17] G. Dong, C. Peng, J. Luo, C. Wang, L. Han, B. Wu, G. Ji, H. He, Adamantane-Resistant Influenza A Viruses in the World (1902–2013): Frequency and Distribution of M2 Gene Mutations, *PLoS One.* 10 (2015) e0119115. doi:10.1371/journal.pone.0119115.
- [18] T. Baranovich, R. Saito, Y. Suzuki, H. Zaraket, C. Dapat, I. Caperig-Dapat, T. Oguma, I.I. Shabana, T. Saito, H. Suzuki, Emergence of H274Y oseltamivir-resistant A(H1N1) influenza viruses in Japan during the 2008–2009 season, *J. Clin. Virol.* 47 (2010) 23–28. doi:10.1016/J.JCV.2009.11.003.
- [19] M. Okomo-Adhiambo, K. Sleeman, K. Ballenger, H.T. Nguyen, V.P. Mishin, T.G. Sheu, J. Smagala, Y. Li, A.I. Klimov, L. V. Gubareva, Neuraminidase Inhibitor Susceptibility Testing in Human

- Influenza Viruses: A Laboratory Surveillance Perspective, *Viruses*. 2 (2010) 2269–2289. doi:10.3390/v2102269.
- [20] R.A. Bright, M. Medina, X. Xu, G. Perez-Oronoz, T.R. Wallis, X.M. Davis, L. Povinelli, N.J. Cox, A.I. Klimov, Incidence of adamantane resistance among influenza A (H3N2) viruses isolated worldwide from 1994 to 2005: a cause for concern, *Lancet*. 366 (2005) 1175–1181. doi:10.1016/S0140-6736(05)67338-2.
- [21] C. Cheung, J.M. Rayner, G.J.D. Smith, P. Wang, T.S.P. Naipospos, J. Zhang, K. Yuen, R.G. Webster, J.S.M. Peiris, Y. Guan, H. Chen, Distribution of Amantadine- Resistant H5N1 Avian Influenza Variants in Asia, *J. Infect. Dis.* 193 (2006) 1626–1629. doi:10.1086/504723.
- [22] I.G. Barr, A.C. Hurt, P. Iannello, C. Tomasov, N. Deed, N. Komadina, Increased adamantane resistance in influenza A(H3) viruses in Australia and neighbouring countries in 2005, *Antiviral Res.* 73 (2007) 112–117. doi:10.1016/j.antiviral.2006.08.002.
- [23] M.G. Alves Galvão, M.A. Augusta Rocha Crispino Santos, A.J.L. Alves da Cunha, Amantadine and rimantadine for influenza A in children and the elderly, *Cochrane Database Syst. Rev.* 11 (2014) 11–13. doi:10.1002/14651858.CD002745.pub4.
- [24] J. Dunning, J.K. Baillie, B. Cao, F.G. Hayden, International Severe Acute Respiratory and Emerging Infection Consortium (ISARIC), Antiviral combinations for severe influenza., *Lancet. Infect. Dis.* 14 (2014) 1259–70. doi:10.1016/S1473-3099(14)70821-7.
- [25] N. Hengrung, K. El Omari, I. Serna Martin, F.T. Vreede, S. Cusack, R.P. Rambo, C. Vornrhein, G. Bricogne, D.I. Stuart, J.M. Grimes, E. Fodor, Crystal structure of the RNA-dependent RNA polymerase from influenza C virus, *Nature*. 527 (2015) 114–117. doi:10.1038/nature15525.
- [26] S. Reich, D. Guilligay, A. Pflug, H. Malet, I. Berger, T. Crépin, D. Hart, T. Lunardi, M. Nanao, R.W.H. Ruigrok, S. Cusack, Structural insight into cap-snatching and RNA synthesis by influenza polymerase, *Nature*. 516 (2014) 361–366. doi:10.1038/nature14009.
- [27] M. Yamashita, M. Krystal, P. Palese, Comparison of the three large polymerase proteins of influenza A, B, and C viruses, *Virology*. 171 (1989) 458–466. doi:10.1016/0042-6822(89)90615-6.
- [28] J.K. Taubenberger, J.C. Kash, Influenza Virus Evolution, Host Adaptation, and Pandemic Formation, *Cell Host Microbe*. 7 (2010) 440–451. doi:10.1016/J.CHOM.2010.05.009.
- [29] A. Stevaert, L. Naesens, The Influenza Virus Polymerase Complex : An Update on Its Structure , Functions , and Significance for Antiviral Drug Design, *Med. Res. Rev.* 36 (2016) 1–47. doi:10.1002/med.21401.
- [30] L. Naesens, A. Stevaert, E. Vanderlinden, Antiviral therapies on the horizon for influenza, *Curr. Opin. Pharmacol.* 30 (2016) 106–115. doi:10.1016/J.COPH.2016.08.003.
- [31] J.S.M. Peiris, M.D. de Jong, Y. Guan, Avian Influenza Virus (H5N1): a Threat to Human Health, *Clin. Microbiol. Rev.* 20 (2007) 243–267. doi:10.1128/CMR.00037-06.
- [32] A. Loregian, B. Mercorelli, G. Nannetti, C. Compagnin, G. Palù, Antiviral strategies against influenza virus: towards new therapeutic approaches, *Cell. Mol. Life Sci.* 71 (2014) 3659–3683.

doi:10.1007/s00018-014-1615-2.

- [33] Y. Kawaoka, *Influenza Virology: Current Topics*, Caister Academic Press, 2006.
- [34] A. Mikulášová, E. Varecková, E. Fodor, Transcription and replication of the influenza A virus genome., *Acta Virol.* 44 (2000) 273–82.
- [35] G. Neumann, G.G. Brownlee, E. Fodor, Y. Kawaoka, Orthomyxovirus replication, transcription, and polyadenylation., *Curr. Top. Microbiol. Immunol.* 283 (2004) 121–43.
- [36] M.A. Horisberger, The large P proteins of influenza A viruses are composed of one acidic and two basic polypeptides., *Virology.* 107 (1980) 302–5.
- [37] J. Braam, I. Ulmanen, R.M. Krug, Molecular model of a eucaryotic transcription complex: functions and movements of influenza P proteins during capped RNA-primed transcription., *Cell.* 34 (1983) 609–18.
- [38] K. Nagata, A. Kawaguchi, T. Naito, Host factors for replication and transcription of the influenza virus genome, *Rev. Med. Virol.* 18 (2008) 247–260. doi:10.1002/rmv.575.
- [39] B. Perales, J. Ortín, The influenza A virus PB2 polymerase subunit is required for the replication of viral RNA., *J. Virol.* 71 (1997) 1381–5.
- [40] M.-T.M. Lee, K. Klumpp, P. Digard, L. Tiley, Activation of influenza virus RNA polymerase by the 5' and 3' terminal duplex of genomic RNA., *Nucleic Acids Res.* 31 (2003) 1624–32.
- [41] A. Pflug, D. Guilligay, S. Reich, S. Cusack, Structure of influenza A polymerase bound to the viral RNA promoter, *Nature.* 516 (2014) 355–360. doi:10.1038/nature14008.
- [42] T. Deng, J.L. Sharps, G.G. Brownlee, G.G. Brownlee Correspondence, G.G. Brownlee, S. William, Role of the influenza virus heterotrimeric RNA polymerase complex in the initiation of replication, *J. Gen. Virol.* 87 (2006) 3373–3377. doi:10.1099/vir.0.82199-0.
- [43] S.J. Plotch, M. Bouloy, I. Ulmanen, R.M. Krug, A unique cap(m7GpppXm)-dependent influenza virion endonuclease cleaves capped RNAs to generate the primers that initiate viral RNA transcription., *Cell.* 23 (1981) 847–58.
- [44] E. Obayashi, H. Yoshida, F. Kawai, N. Shibayama, A. Kawaguchi, K. Nagata, J.R.H. Tame, S.-Y. Park, The structural basis for an essential subunit interaction in influenza virus RNA polymerase, (n.d.). doi:10.1038/nature07225.
- [45] A. Kawaguchi, T. Naito, K. Nagata, Involvement of influenza virus PA subunit in assembly of functional RNA polymerase complexes., *J. Virol.* 79 (2005) 732–44. doi:10.1128/JVI.79.2.732-744.2005.
- [46] E. Fodor, L.J. Mingay, M. Crow, T. Deng, G.G. Brownlee, A single amino acid mutation in the PA subunit of the influenza virus RNA polymerase promotes the generation of defective interfering RNAs., *J. Virol.* 77 (2003) 5017–20. doi:10.1128/JVI.77.8.5017-5020.2003.
- [47] A. York, E. Fodor, Biogenesis, assembly, and export of viral messenger ribonucleoproteins in the influenza A virus infected cell., *RNA Biol.* 10 (2013) 1274–82. doi:10.4161/rna.25356.
- [48] P. Resa-Infante, N. Jorba, R. Coloma, J. Ortin, The influenza virus RNA synthesis machine: advances

in its structure and function., *RNA Biol.* 8 (2011) 207–15. doi:10.4161/RNA.8.2.14513.

- [49] Z. Zhou, T. Liu, J. Zhang, P. Zhan, X. Liu, Influenza A virus polymerase: an attractive target for next-generation anti-influenza therapeutics, *Drug Discov. Today.* (2018). doi:10.1016/j.drudis.2018.01.028.
- [50] G. Muratore, L. Goracci, B. Mercorelli, Á. Foeglein, P. Digard, G. Cruciani, G. Palù, A. Loregian, Small molecule inhibitors of influenza A and B viruses that act by disrupting subunit interactions of the viral polymerase, *Proc. Natl. Acad. Sci. U. S. A.* 109 (2012) 6247. doi:10.1073/PNAS.1119817109.
- [51] B. Mänz, V. Götz, K. Wunderlich, J. Eisel, J. Kirchmair, J. Stech, O. Stech, G. Chase, R. Frank, M. Schwemmler, Disruption of the viral polymerase complex assembly as a novel approach to attenuate influenza A virus., *J. Biol. Chem.* 286 (2011) 8414–24. doi:10.1074/jbc.M110.205534.
- [52] S. Massari, L. Goracci, J. Desantis, O. Tabarrini, Polymerase Acidic Protein–Basic Protein 1 (PA–PB1) Protein–Protein Interaction as a Target for Next-Generation Anti-influenza Therapeutics, *J. Med. Chem.* 59 (2016) 7699–7718. doi:10.1021/acs.jmedchem.5b01474.
- [53] A. Ghanem, D. Mayer, G. Chase, W. Tegge, R. Frank, G. Kochs, A. Garcia-Sastre, M. Schwemmler, Peptide-Mediated Interference with Influenza A Virus Polymerase, *J. Virol.* 81 (2007) 7801–7804. doi:10.1128/JVI.00724-07.
- [54] H. Liu, X. Yao, Molecular Basis of the Interaction for an Essential Subunit PA–PB1 in Influenza Virus RNA Polymerase: Insights from Molecular Dynamics Simulation and Free Energy Calculation, *Mol. Pharm.* 7 (2010) 75–85. doi:10.1021/mp900131p.
- [55] D. Rognan, Rational design of protein–protein interaction inhibitors, *Medchemcomm.* 6 (2015) 51–60. doi:10.1039/C4MD00328D.
- [56] K. Wunderlich, D. Mayer, C. Ranadheera, A.-S. Holler, B. Mänz, A. Martin, G. Chase, W. Tegge, R. Frank, U. Kessler, M. Schwemmler, Identification of a PA-binding peptide with inhibitory activity against influenza A and B virus replication., *PLoS One.* 4 (2009) e7517. doi:10.1371/journal.pone.0007517.
- [57] S. Massari, G. Nannetti, L. Goracci, L. Sancineto, G. Muratore, S. Sabatini, G. Manfroni, B. Mercorelli, V. Cecchetti, M. Facchini, G. Palù, G. Cruciani, A. Loregian, O. Tabarrini, Structural Investigation of Cycloheptathiophene-3-carboxamide Derivatives Targeting Influenza Virus Polymerase Assembly, *J. Med. Chem.* 56 (2013) 10118–10131. doi:10.1021/jm401560v.
- [58] S. Massari, G. Nannetti, J. Desantis, G. Muratore, S. Sabatini, G. Manfroni, B. Mercorelli, V. Cecchetti, G. Palù, G. Cruciani, A. Loregian, L. Goracci, O. Tabarrini, A Broad Anti-influenza Hybrid Small Molecule That Potently Disrupts the Interaction of Polymerase Acidic Protein–Basic Protein 1 (PA–PB1) Subunits, *J. Med. Chem.* 58 (2015) 3830–3842. doi:10.1021/acs.jmedchem.5b00012.
- [59] M. Fukuoka, M. Minakuchi, A. Kawaguchi, K. Nagata, Y.O. Kamatari, K. Kuwata, Structure-based discovery of anti-influenza virus A compounds among medicines., *Biochim. Biophys. Acta.* 1820 (2012) 90–5. doi:10.1016/j.bbagen.2011.11.003.
- [60] G. Muratore, B. Mercorelli, L. Goracci, G. Cruciani, P. Digard, G. Palù, A. Loregian, Human cytomegalovirus inhibitor AL18 also possesses activity against influenza A and B viruses., *Antimicrob.*

Agents Chemother. 56 (2012) 6009–13. doi:10.1128/AAC.01219-12.

- [61] C. Li, Q. Ba, A. Wu, H. Zhang, T. Deng, T. Jiang, A peptide derived from the C-terminus of PB1 inhibits influenza virus replication by interfering with viral polymerase assembly, *FEBS J.* 280 (2013) 1139–1149. doi:10.1111/febs.12107.
- [62] G. Chase, K. Wunderlich, P. Reuther, M. Schwemmle, Identification of influenza virus inhibitors which disrupt of viral polymerase protein–protein interactions, *Methods.* 55 (2011) 188–191. doi:10.1016/j.ymeth.2011.08.007.
- [63] C. Tintori, I. Laurenzana, A.L. Fallacara, U. Kessler, B. Pilger, L. Stergiou, M. Botta, High-throughput docking for the identification of new influenza A virus polymerase inhibitors targeting the PA–PB1 protein–protein interaction, *Bioorg. Med. Chem. Lett.* 24 (2014) 280–282. doi:10.1016/j.bmcl.2013.11.019.
- [64] S. Yuan, H. Chu, H. Zhao, K. Zhang, K. Singh, B.K.C. Chow, R.Y.T. Kao, J. Zhou, B.-J. Zheng, Identification of a small-molecule inhibitor of influenza virus via disrupting the subunits interaction of the viral polymerase, *Antiviral Res.* 125 (2016) 34–42. doi:10.1016/j.antiviral.2015.11.005.
- [65] S. Lepri, G. Nannetti, G. Muratore, G. Cruciani, R. Ruzziconi, B. Mercorelli, G. Palù, A. Loregian, L. Goracci, Optimization of Small-Molecule Inhibitors of Influenza Virus Polymerase: From Thiophene-3-Carboxamide to Polyamido Scaffolds, *J. Med. Chem.* 57 (2014) 4337–4350. doi:10.1021/jm500300r.
- [66] U. Kessler, D. Castagnolo, M. Pagano, D. Deodato, M. Bernardini, B. Pilger, C. Ranadheera, M. Botta, Discovery and synthesis of novel benzofurazan derivatives as inhibitors of influenza A virus., *Bioorg. Med. Chem. Lett.* 23 (2013) 5575–7. doi:10.1016/j.bmcl.2013.08.048.
- [67] M. Pagano, D. Castagnolo, M. Bernardini, A.L. Fallacara, I. Laurenzana, D. Deodato, U. Kessler, B. Pilger, L. Stergiou, S. Strunze, C. Tintori, M. Botta, The Fight against the Influenza A Virus H1N1: Synthesis, Molecular Modeling, and Biological Evaluation of Benzofurazan Derivatives as Viral RNA Polymerase Inhibitors, *ChemMedChem.* 9 (2014) 129–150. doi:10.1002/cmdc.201300378.
- [68] X. He, J. Zhou, M. Bartlam, R. Zhang, J. Ma, Z. Lou, X. Li, J. Li, A. Joachimiak, Z. Zeng, R. Ge, Z. Rao, Y. Liu, Crystal structure of the polymerase PAC–PB1N complex from an avian influenza H5N1 virus, *Nature.* 454 (2008) 1123–1126. doi:10.1038/nature07120.
- [69] R.A. Friesner, J.L. Banks, R.B. Murphy, T.A. Halgren, J.J. Klicic, D.T. Mainz, M.P. Repasky, E.H. Knoll, M. Shelley, J.K. Perry, D.E. Shaw, P. Francis, P.S. Shenkin, D.E.S. Research, Glide: A New Approach for Rapid, Accurate Docking and Scoring. 1. Method and Assessment of Docking Accuracy, (n.d.). doi:10.1021/jm0306430.
- [70] M.L. Verdonk, J.C. Cole, M.J. Hartshorn, C.W. Murray, R.D. Taylor, Improved protein–ligand docking using GOLD, *Proteins Struct. Funct. Bioinforma.* 52 (2003) 609–623. doi:10.1002/prot.10465.
- [71] I.M.L. Trist, G. Nannetti, C. Tintori, A.L. Fallacara, D. Deodato, B. Mercorelli, G. Palu, M. Wijtmans, T. Gospodova, E. Edink, M. Verheij, I. De Esch, L. Viteva, A. Loregian, M. Botta, 4,6-Diphenylpyridines as Promising Novel Anti-Influenza Agents Targeting the PA – PB1 Protein – Protein Interaction: Structure – Activity Relationships Exploration with the Aid of Molecular

Modeling, (2016). doi:10.1021/acs.jmedchem.5b01935.

- [72] N.J. Yang, M.J. Hinner, Getting across the cell membrane: an overview for small molecules, peptides, and proteins., *Methods Mol. Biol.* 1266 (2015) 29–53. doi:10.1007/978-1-4939-2272-7_3.
- [73] K. Beaumont, R. Webster, I. Gardner, K. Dack, Design of Ester Prodrugs to Enhance Oral Absorption of Poorly Permeable Compounds: Challenges to the Discovery Scientist, *Curr. Drug Metab.* 4 (2003) 461–485. doi:10.2174/1389200033489253.
- [74] K. Wunderlich, M. Juozapaitis, C. Ranadheera, U. Kessler, A. Martin, J. Eisel, U. Beutling, R. Frank, M. Schwemmle, Identification of high-affinity PB1-derived peptides with enhanced affinity to the PA protein of influenza A virus polymerase., *Antimicrob. Agents Chemother.* 55 (2011) 696–702. doi:10.1128/AAC.01419-10.
- [75] J. Montes-Avila, S.P. Díaz-Camacho, J. Sicairos-Félix, F. Delgado-Vargas, I.A. Rivero, Solution-phase parallel synthesis of substituted chalcones and their antiparasitary activity against *Giardia lamblia*, *Bioorg. Med. Chem.* 17 (2009) 6780–6785. doi:10.1016/j.bmc.2009.02.052.
- [76] A.N. Choudhary, V. Juyal, Synthesis of chalcone and their derivatives as antimicrobial agents. *International Journal of Pharmacy and Pharmaceutical Sciences.* 2011; 3:125-128.
- [77] F. Hayat, A. Salahuddin, S. Umar, A. Azam, Synthesis, characterization, antiamoebic activity and cytotoxicity of novel series of pyrazoline derivatives bearing quinoline tail, *Eur. J. Med. Chem.* 45 (2010) 4669–4675. doi:10.1016/J.EJMECH.2010.07.028.
- [78] A.M. Attia, G.H. Elgemeie, A New Class of Dihydropyridine Thioglycosides via Piperidinium Salts, *Synth. Commun.* 33 (2003) 2243–2255. doi:10.1081/SCC-120021503.
- [79] X.-Q. Zhu, B.-J. Zhao, J.-P. Cheng, Mechanisms of the Oxidations of NAD(P)H Model Hantzsch 1,4-Dihydropyridines by Nitric Oxide and Its Donor N-Methyl-N-nitrosotoluene-p-sulfonamide, (2000). doi:10.1021/JO000484H.
- [80] G. Windridge, E.C. Jorgensen, 1-Hydroxybenzotriazole as a racemization-suppressing reagent for the incorporation of im-benzyl-L-histidine into peptides, *J. Am. Chem. Soc.* 93 (1971) 6318–6319. doi:10.1021/ja00752a081.
- [81] R.W. Sidwell, J.H. Huffman, G.P. Khare, L.B. Allen, J.T. Witkowski, R.K. Robins, Broad-spectrum antiviral activity of Virazole: 1-beta-D-ribofuranosyl-1,2,4-triazole-3-carboxamide., *Science.* 177 (1972) 705–6.
- [82] G. Jones, P. Willett, R.C. Glen, A.R. Leach, R. Taylor, Development and validation of a genetic algorithm for flexible docking 1 Edited by F. E. Cohen, *J. Mol. Biol.* 267 (1997) 727–748. doi:10.1006/jmbi.1996.0897.
- [83] Y. Cau, M. Mori, C.T. Supuran, M. Botta, Mycobacterial carbonic anhydrase inhibition with phenolic acids and esters: kinetic and computational investigations, *Org. Biomol. Chem.* 14 (2016) 8322–8330. doi:10.1039/C6OB01477A.
- [84] Y. Cau, A. Fiorillo, M. Mori, A. Ilari, M. Botta, M. Lalle, Molecular Dynamics Simulations and Structural Analysis of *Giardia duodenalis* 14-3-3 Protein–Protein Interactions, *J. Chem. Inf. Model.* 55

(2015) 2611–2622. doi:10.1021/acs.jcim.5b00452.

- [85] B.R. Miller, T.D. McGee, J.M. Swails, N. Homeyer, H. Gohlke, A.E. Roitberg, *MMPBSA.py*: An Efficient Program for End-State Free Energy Calculations, *J. Chem. Theory Comput.* 8 (2012) 3314–3321. doi:10.1021/ct300418h.
- [86] D.A. Case et al (2016), AMBER 2016, University of California, San Francisco.
- [87] D.R. Roe, T.E. Cheatham, PTRAJ and CPPTRAJ: Software for Processing and Analysis of Molecular Dynamics Trajectory Data, *J. Chem. Theory Comput.* 9 (2013) 3084–3095. doi:10.1021/ct400341p.
- [88] A. Loregian, B.A. Appleton, J.M. Hogle, D.M. Coen, Residues of human cytomegalovirus DNA polymerase catalytic subunit UL54 that are necessary and sufficient for interaction with the accessory protein UL44., *J. Virol.* 78 (2004) 158–67. doi:10.1128/JVI.78.1.158-167.2004.
- [89] J. Desantis, G. Nannetti, S. Massari, M. Letizia, G. Manfroni, V. Cecchetti, G. Palù, L. Goracci, A. Loregian, O. Tabarrini, European Journal of Medicinal Chemistry Exploring the cycloheptathiophene-3-carboxamide scaffold to disrupt the interactions of the in fl uenza polymerase subunits and obtain potent anti-in fl uenza activity, *Eur. J. Med. Chem.* 138 (2017) 128–139. doi:10.1016/j.ejmech.2017.06.015.
- [90] A. Loregian, D.M. Coen, Selective Anti-Cytomegalovirus Compounds Discovered by Screening for Inhibitors of Subunit Interactions of the Viral Polymerase, *Chem. Biol.* 13 (2006) 191–200. doi:10.1016/j.chembiol.2005.12.002.
- [91] S. Massari, J. Desantis, G. Nannetti, S. Sabatini, S. Tortorella, L. Goracci, V. Cecchetti, A. Loregian, O. Tabarrini, Efficient and regioselective one-step synthesis of 7-aryl-5-methyl- and 5-aryl-7-methyl-2-amino-[1,2,4]triazolo[1,5-a]pyrimidine derivatives, *Org. Biomol. Chem.* 15 (2017) 7944–7955. doi:10.1039/C7OB02085F.
- [92] A.E. Mullin, R.M. Dalton, M.J. Amorim, D. Elton, P.D. Correspondence, P. Digard, Increased amounts of the influenza virus nucleoprotein do not promote higher levels of viral genome replication, (n.d.). doi:10.1099/vir.0.80518-0.
- [93] J.B. Baell, G.A. Holloway, New Substructure Filters for Removal of Pan Assay Interference Compounds (PAINS) from Screening Libraries and for Their Exclusion in Bioassays, *J. Med. Chem.* 53 (2010) 2719–2740. doi:10.1021/jm901137j.
- [94] B. Neron, H. Menager, C. Maufrais, N. Joly, J. Maupetit, S. Letort, S. Carrere, P. Tuffery, C. Letondal, Mobylye: a new full web bioinformatics framework, *Bioinformatics.* 25 (2009) 3005–3011. doi:10.1093/bioinformatics/btp493.
- [95] C. Alland, F. Moreews, D. Boens, M. Carpentier, S. Chiusa, M. Lonquety, N. Renault, Y. Wong, H. Cantalloube, J. Chomilier, J. Hochez, J. Pothier, B.O. Villoutreix, J.-F. Zagury, P. Tuffery, RPBS: a web resource for structural bioinformatics, *Nucleic Acids Res.* 33 (2005) W44–W49. doi:10.1093/nar/gki477.
- [96] D. Lagorce, O. Sperandio, J.B. Baell, M.A. Miteva, B.O. Villoutreix, FAF-Drugs3: a web server for compound property calculation and chemical library design, *Nucleic Acids Res.* 43 (2015) W200–

W207. doi:10.1093/nar/gkv353.

- [97] FAF-Drugs3 Free ADME/tox Filtering tool 4. <http://fafdrugs3.mti.univ-paris-diderot.fr>. Accessed in March 2018.